Ecological Engineering 210 (2025) 107439

Contents lists available at ScienceDirect

Ecological Engineering

journal homepage: www.elsevier.com/locate/ecoleng

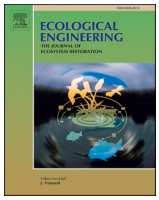

Nature-based mitigation of shoreline erosion risks in tidal marshes created by managed realignment vs. sediment nourishment

Marte M. Stoorvogel [a,b,*], Pim W.J.M. Willemsen [c,d], Jim van Belzen [a,e], Stijn Temmerman [f], Jan M. de Jonge [g], Johan van de Koppel [a,h], Tjeerd J. Bouma [a,b]

[a] Department of Estuarine and Delta Systems, NIOZ Royal Netherlands Institute for Sea Research, Korringaweg 7, 4401 NT Yerseke, the Netherlands
[b] Department of Physical Geography, Utrecht University, Princetonlaan 8a, 3584 CB Utrecht, the Netherlands
[c] Hydrology and Environmental Hydraulics Group, Department of Environmental Sciences, Wageningen University & Research, Droevendaalsesteeg 4, 6708 PB Wageningen, the Netherlands
[d] Department of Ecosystems and Sediment Dynamics, Deltares, Boussinesqweg 1, 2629 HV Delft, the Netherlands
[e] Wageningen Marine Research, Wageningen University & Research, Korringaweg 7, 4401 NT Yerseke, the Netherlands
[f] ECOSPHERE Research Group, Department of Biology, University of Antwerp, Groenenborgerlaan 171, 2020 Antwerp, Belgium
[g] Department of Chemical Engineering, TU Delft, Van der Maasweg 9, 2629 HZ Delft, the Netherlands
[h] Conservation Ecology Group, Groningen Institute for Evolutionary Life Sciences, University of Groningen, Nijenborgh 7, 9747 AG Groningen, the Netherlands

ARTICLE INFO

Keywords:
Nature-based flood defence
Nature-based solutions
Sediment strength
Sediment stability
Vegetation establishment
Sediment grain size
Tidal inundation

ABSTRACT

Tidal marshes provide many valuable ecosystem services and can play an important role in nature-based flood risk mitigation along low-lying coasts and estuaries, by attenuating waves and increasing erosion resistance. There is an effort around the world to restore or create tidal marshes, but it remains unknown how different marsh restoration and creation techniques affect the development of erosion resistant sediment beds, which is essential for their contribution to long-term erosion and flood risk mitigation. Here, we compared sediment shear strength and erosion resistance under very high flow velocity (i.e. as may occur during the breach of a dike or seawall behind the marsh) of a managed realignment site versus a sediment nourishment site, restored and created respectively, and assessed the effects of tidal inundation, sediment characteristics, and vegetation. Managed realignment consists of the landward relocation of flood defence structures like seawalls and dikes and tidal flooding of low-lying land, creating a sheltered environment for tidal deposition of fine-grained sediments, while sediment nourishment is the seaward placement of mostly more coarse-grained dredged sediment. This study showed that at both sites sediment shear strength and erosion resistance were higher at vegetated locations than at unvegetated locations. In addition, at the managed realignment site, tidal inundation duration affected shear strength negatively, while bulk density affected shear strength positively. At the sediment nourishment site, sediment grain size was the most important driving factor of shear strength and erosion resistance, besides vegetation presence: a decreasing shear strength and erosion resistance were observed with increasing sediment grain size. Managed realignment and sediment nourishment both have advantages and disadvantages for the fast development of an erosion resistant sediment bed. Managed realignment will likely lead to fine-grained, cohesive sediments, which are in this case colonised by dense, but slowly establishing, mud-loving *Spartina* vegetation. In contrast, sediment nourishments are typically done with more coarse-grained, non-cohesive sediments, which are in this case colonised by initially sparse, fast establishing *Salicornia* vegetation. Dense *Spartina* increased erosion resistance more than sparse *Salicornia*. If we plan well ahead of time and temporarily support their development, restored or created marshes have time to become erosion resistant, thereby enabling sustainable use of marsh ecosystem services for long-term nature-based flood risk mitigation.

* Corresponding author at: Department of Estuarine and Delta Systems, NIOZ Royal Netherlands Institute for Sea Research, Korringaweg 7, 4401 NT Yerseke, the Netherlands.

E-mail addresses: marte.stoorvogel@nioz.nl (M.M. Stoorvogel), pim.willemsen@wur.nl (P.W.J.M. Willemsen), jim.van.belzen@nioz.nl (J. van Belzen), stijn.temmerman@uantwerpen.be (S. Temmerman), johan.van.de.koppel@nioz.nl (J. van de Koppel), tjeerd.bouma@nioz.nl (T.J. Bouma).

https://doi.org/10.1016/j.ecoleng.2024.107439
Received 4 July 2024; Received in revised form 20 September 2024; Accepted 2 November 2024
Available online 16 November 2024

1. Introduction

Tidal marshes are intertidal wetlands that provide many valuable ecosystem services, such as carbon sequestration (Duarte et al., 2013; Rogers et al., 2019; Temmink et al., 2022), water purification (Nelson and Zavaleta, 2012), habitat provisioning (Spencer and Harvey, 2012), coastal erosion prevention (Lo et al., 2017; Wang et al., 2017), and recreational activities (Barbier et al., 2011). It is increasingly recognized that tidal marshes can also play an important role in flood risk mitigation along coastal and estuarine shorelines. Their vegetated surface and erosion resistant, elevated surface bed attenuate waves (Marin-Diaz et al., 2023; Möller et al., 2014; Zhu et al., 2020) and reduce storm surge heights (Fairchild et al., 2021; Smolders et al., 2015), thereby reducing dike breach probabilities along shorelines where dikes are used for flood risk mitigation (Vuik et al., 2016; Zhu et al., 2020). Moreover, in the extreme case that a dike breach would occur, an elevated, erosion resistant marsh bed in front of a dike reduces the breach dimensions and thereby results in a slower water level rise behind the breach, which would lead to less damage and casualties (van den Hoven et al., 2023; Zhu et al., 2020). Furthermore, one of the major advantages of using tidal marshes for nature-based flood risk mitigation is that marshes can grow with sea-level rise (Coleman et al., 2022; Fagherazzi et al., 2012; Temmerman et al., 2023). This climate-proofs their flood defence values and makes climate adaptation more affordable compared to engineered flood defences such as dikes that need regular, costly maintenance (van Zelst et al., 2021). Unfortunately, many tidal marshes are under pressure due to erosion and decreasing sediment supplies because of dam and barrier construction (Doody, 2013; Kirwan and Megonigal, 2013). However, with increasing recognition of tidal marsh services (Barbier et al., 2011) and the growing need for affordable flood defences that are able to adapt to the consequences of climate change (e.g. sea-level rise; van Zelst et al., 2021), there is a global effort to restore and create tidal marshes for nature-based flood risk mitigation (ABPmer, 2024; Gourgue et al., 2022).

Many different techniques for tidal marsh restoration and creation exist, and their suitability depends on the location and goal. What all restoration and creation approaches have in common is that they aim to provide a wave-sheltered, high intertidal bed surface elevation, and thereby create disturbance free 'Windows of Opportunity' that allow plant seedling establishment (Balke et al., 2014; Hu et al., 2015). Marsh restoration on historically embanked, low-lying land (i.e. landward of original flood defences) can be done by (1) managed realignment (ABPmer, 2024), where a previously embanked area is exposed again to the tides by building new flood defences (e.g. dikes) more inland and removing or breaching part of the original flood defences (French, 2006). A similar option for marsh restoration on low-lying embanked land is (2) regulated tidal exchange, where the original dike is kept in place and tidal exchange occurs through structures (e.g. sluices or culverts) built in the original flood defences (Maris et al., 2007; Temmerman et al., 2013; Wolters et al., 2005). This enables control over the tidal regime in the restored area. Marsh habitat creation seaward in front of flood defences, at locations where no marsh has occurred in the past, can be achieved by a range of techniques. One of these is (3) aiming to reduce hydrodynamics by placing brushwood groynes (i.e. an often temporary and relatively low (typically $<$1.5 m) wave-attenuating structure made by tying wooden branches horizontally in between vertical wooden poles that are placed deep into the sediment for stability; Winterwerp et al., 2020), oyster or mussel reefs, or stone or concreate dams, to enhance sediment accumulation and thus increase bed surface elevation to stimulate tidal marsh development (e.g. De Groot and Van Duin, 2013; Dijkema et al., 2007; Gedan et al., 2011). Further, (4) sediment nourishment to raise bed surface elevation at too low areas, by applying dredged material, could create a suitable environment for vegetation establishment (De Groot and Van Duin, 2013). Once the bed is elevated, marsh development can be further enhanced by seeding salt marsh vegetation (Baptist et al., 2021). Whereas all these four techniques can be used for tidal marsh restoration or creation, the resulting marshes will only be able to contribute significantly to long-term flood risk mitigation if their sediment beds become erosion resistant, also under the high flow velocities associated with the breach of a dike or seawall behind the marsh.

Mature tidal marsh sediment beds have been shown to be erosion resistant, both under wave attacks (Möller et al., 2014; Wang et al., 2017) and under high flow velocities (Marin-Diaz et al., 2022; Schoutens et al., 2022). During tidal marsh development, erosion resistance of sediment beds can increase through several processes. The *first* is sediment consolidation (i.e. increase in sediment strength), where sediment particles form a denser structure as pore water is expelled from the sediment matrix (Torfs et al., 1996). This leads to an increase in bulk density (Colosimo et al., 2023), and thereby an increase in erosion resistance (Chen et al., 2012; Grabowski et al., 2011; Zhou et al., 2016). Sediment consolidation can happen due to the weight of newly deposited sediment on top, called self-weight consolidation (Barciela-Rial et al., 2020; Zhou et al., 2016), and through drying out of the sediment, called drying-induced consolidation (Colosimo et al., 2023; Dong et al., 2020). A *second* process that can increase erosion resistance is the accumulation of fine-grained cohesive particles, such as clay and silt particles, that are supplied with the flooding tides as suspended particulate matter (Brooks et al., 2021; Grabowski et al., 2011). Plants can contribute to fine-grained suspended sediment deposition by 1) directly capturing the suspended particles on plant structures and by 2) reducing flow velocities and thereby increasing suspended particle settling rates (Fagherazzi et al., 2012). *Third*, vegetation growth generally leads to an increase in erosion resistance. Once seedlings establish on bare tidal flats, their roots will start to increase erosion resistance by binding the sediment (Chen et al., 2012; Lo et al., 2017; Wang et al., 2017). Increasing root biomass was found to decrease sediment erodibility (Ford et al., 2016; Wang et al., 2017).

Although these mechanistic insights into the development of erosion resistance of marsh sediment beds exist, a comparison of the development of sediment strength and erosion resistance under high flow velocity (i.e. as may occur during the breach of a dike or seawall behind the marsh) between different marsh restoration and creation techniques remains lacking. In addition, it is unknown which other site-dependent factors drive the development of sediment strength and erosion resistance in restored and created tidal marshes. The lack of this knowledge results in the inability to quantify the long-term effectiveness of restored or created tidal marshes for the purpose of flood risk mitigation. Our aim is therefore to improve our current understanding of the development of sediment strength and erosion resistance under a high flow velocity in restored and created tidal marshes, and of how this development is affected by tidal inundation, sediment characteristics, and vegetation. For this, we compared sediment strength and erosion resistance at a managed realignment site (since 2015) and at a sediment nourishment site combined with brushwood groynes (since 2018). At both these sites, we selected locations with differences in tidal inundation duration, sediment grain size, and vegetation presence or absence, to test the effect of these factors on sediment strength and erosion resistance.

2. Methods

2.1. Studied tidal marshes

We conducted our study at two tidal marshes in the Netherlands; the managed realignment site Perkpolder in the Western Scheldt estuary (SW Netherlands) and the sediment nourishment site Marconi in the Ems-Dollard estuary (NE Netherlands; Fig. 1).

Perkpolder is a managed realignment site of 75 ha where a new ring dike was built more landward around the area and the original embankment was breached in June 2015, for the purposes of nature restoration and compensation, flood defence, and recreational activities (Brunetta et al., 2019; Walles et al., 2019). Before de-embankment, the

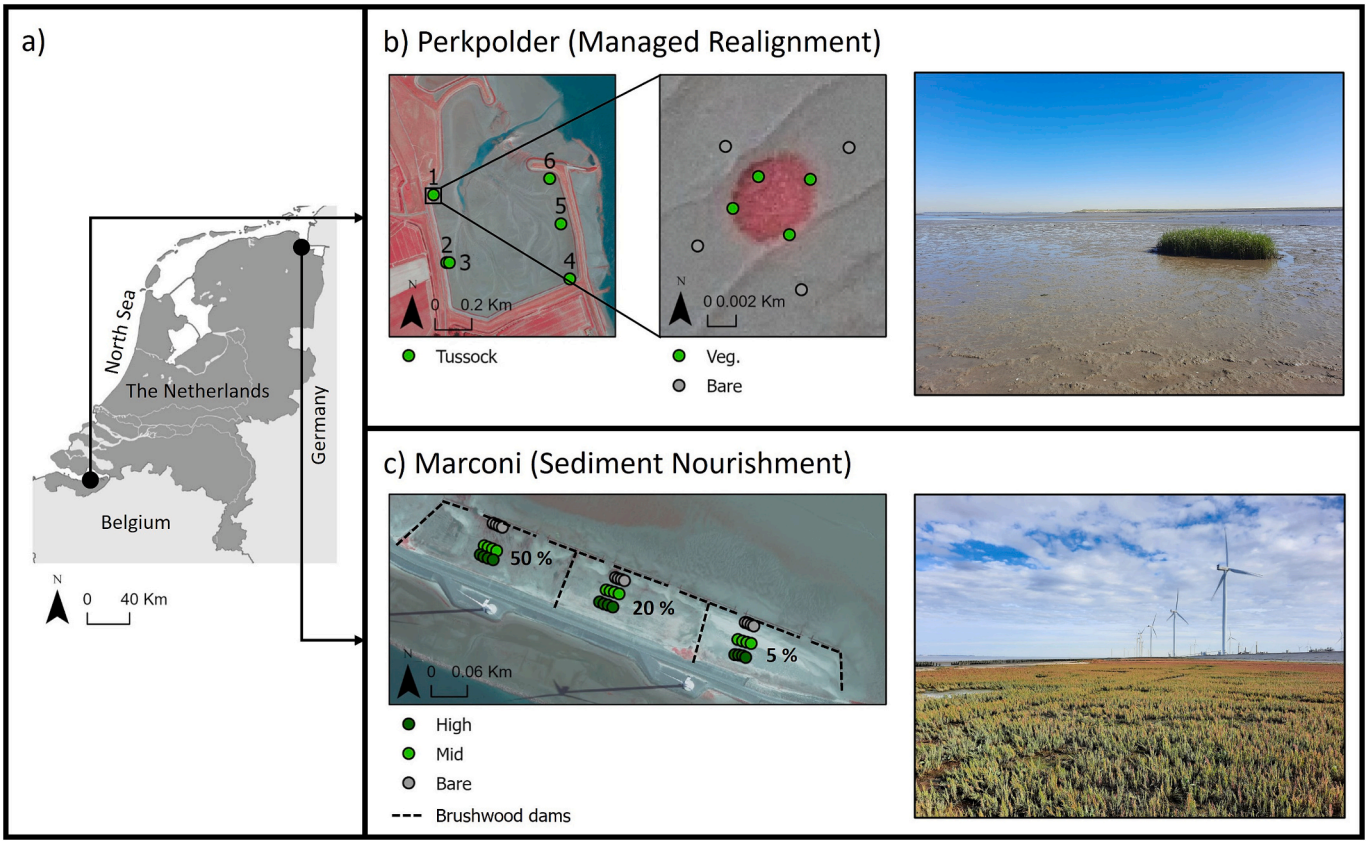

Fig. 1. a) Location of Perkpolder in SW Netherlands and the Marconi Project in NE Netherlands. b) Left: Locations of the studied tussocks at Perkpolder and the four vegetated (veg.) measurement locations in the tussocks and the four bare measurement locations on the tidal flat next to the tussocks. The background map is a false colour aerial image of 2022 (collected by Rijkswaterstaat), with red indicating vegetation. Right: Photo of Perkpolder, showing tussock 3. c) Left: Locations of the sections with 50 %, 20 %, and 5 % fine fraction content at Marconi, and per section the four vegetated high marsh measurement locations, the four vegetated mid marsh measurement locations, and the four bare tidal flat measurement locations. The background map is a false colour aerial image of 2020 (collected by Rijkswaterstaat), with red indicating vegetation. Dashed, black lines indicate the brushwood dams, separating the three sections. Right: Photo of Marconi, section 50 %. (For interpretation of the references to colour in this figure legend, the reader is referred to the web version of this article.)

area was used for agriculture. Below the newly deposited sediment a strongly compacted, relict agricultural soil is still present, which restricts groundwater fluctuations to the newly deposited sediment (Van Putte et al., 2020). During the restoration process several creeks were dug (Brunetta et al., 2019; Walles et al., 2019). Average salinity in the Western Scheldt around Perkpolder ranges between 10 and 18 PSU and bed level changes ranged between 2016 and 2018 between −1.12 m around the creeks and inlet and + 0.34 m on the platforms (Walles et al., 2019). In July 2015, five approximately 6-week-old *Spartina anglica* and *Scirpus maritimus* seedlings, harvested as seeds from tidal marshes in the Western Scheldt, were planted in a 50 × 50 cm quadrat at 15 locations in Perkpolder, and their survival was monitored. By August 2015 all *Scirpus maritimus* seedlings had disappeared, and by September 2017 *Spartina anglica* seedlings only remained at six locations, which had grown into tussocks by September 2023 (when we took our measurements; Fig. 1b). By 2023, natural *Spartina anglica* seed dispersal was also taking place, resulting in newly forming tussocks, especially in the somewhat higher elevated NW corner of Perkpolder. However, by 2023 Perkpolder remained for the largest part an unvegetated tidal flat.

The goal of the overall Marconi Project was to reconnect the city of Delfzijl with the Ems-Dollard estuary and to improve ecological and recreational services. It included the creation of tidal marsh habitat by sediment nourishment, a bird breeding island, a city beach, a boulevard for biking and walking, and a bridge connecting the city with marshes and beach (De Vries et al., 2021; Eems-Dollard 2050, n.d.; Gemeente Eemsdelta, n.d.). Within the Marconi Project, a pilot pioneer marsh of 15 ha was created in 2018 through sediment nourishment, by elevating the bed level of the designated area mainly with sand. The area was split into six sections that were delineated with permeable brushwood groynes. Since the marsh was intended for a pilot study on, among others, the effect of fine fraction content (clay + silt, < 63 μm) on marsh development, dredged fine fraction material was mixed in different percentages (5, 20, and 50 %) with the sand until a depth of 1 m (De Vries et al., 2021). The dredged fine fraction material was ripened (i.e. converted from waterlogged sediments into soil by desiccation and structure development; Vermeulen et al., 2005) in a storage facility on land before mixing with the sand. However, we observed in the field that the sand and fine sediment were not fully mixed, as the sediment in the 20 and 50 % sections consisted of a sand matrix with large blocks (Ø up to 10 cm) of fine fraction sediment in between. We decided to only use the three eastern sections for our study, because the surface area and alongshore width are equal: one with each of the fine fraction contents (Fig. 1c). Bed level changes between 2018 and 2020 in these sections were relatively small at the higher marsh (< 0.50 m), but large at the lower marsh (up to −2.0 m and + 2.0 m) (De Vries et al., 2021). Salinity of the Ems-Dollard at Delfzijl was on average 22 PSU between 1980 and 1990 (Ysebaert et al., 1998). To test the effect of seeding on marsh development, half of our studied sections were sown in May 2019 with fragments of *Salicornia procumbens* that were collected from a nearby marsh (De Vries et al., 2021). However, vegetation cover and species richness did not differ significantly anymore between the seeded and non-seeded areas in 2020, indicating that the effect of seeding was only temporary (De Vries et al., 2021). Where pioneer vegetation was present mainly depended on the magnitude of bed level change during events:

large bed level changes were observed at bare locations and small changes at vegetated locations (Willemsen et al., 2022).

The different restoration or creation techniques of these two tidal marshes enabled us to study if sediment strength and erosion resistance developed differently under these two techniques.

2.2. Measurement locations

At Perkpolder (herein referred to as the Managed Realignment site; MR-site) we placed our measurement locations near the six planted *Spartina anglica* tussocks that survived until September 2023. Inundation duration of these tussocks ranged between 31.2 % (tussock 4) and 43.4 % (tussock 3), allowing us to study the effect of tidal inundation duration on the development of sediment strength and erosion resistance. To also test the effect of vegetation, the measurements and samples were taken with four replicates inside the tussock (at locations which had gotten vegetated with *Spartina anglica* between 2020 and 2022, as derived from false colour aerial images of Rijkswaterstaat) and with four replicates ±1 m outside of the tussock, on the bare tidal flat (Fig. 1b).

At the pilot pioneer marsh of the Marconi Project (herein referred to as the Sediment Nourishment site; SN-site) we took our measurements and samples in the selected three equally-sized sections, with fine fraction contents of 5, 20, and 50 % (herein referred to as sections 5, 20, and 50 %), to investigate the effect of grain size distribution on the development of sediment strength and erosion resistance. The measurement locations were located at the western sides of all sections, which were seeded with *Salicornia procumbens*. It was noted that the non-seeded part had the same vegetation in terms of cover and species. To study the effects of tidal inundation duration and vegetation, we placed measurement locations at two tidal marsh elevations (herein referred to as 'high marsh' and 'mid marsh') and on the bare tidal flat, at each location with four replicates (Fig. 1c).

2.3. Field measurements and sediment sampling

In September 2023 we took measurements at all measurement locations of both the MR- and SN-site. First, we measured bed elevation (m + NAP) with an RTK-DGPS (Trimble, USA). We determined shear strength of both the sediment surface and of deeper sediment layers, which is a measure of sediment strength. The surface measurements were done with a pocket shear vane tester (torvane; Eijkelkamp, The Netherlands), and the measurements at depths of 10, 20, 30, and 40 cm with a field inspection shear vane tester (Eijkelkamp, The Netherlands). If the maximum measurable shear strength was reached with the pocket shear vane tester (3.2 kPa at the MR-site and 21.9 kPa at the SN-site, depending on attachment used) or field inspection shear vane tester (65 kPa at the MR-site and 130 kPa at the SN-site, depending on attachment used), this shear strength value was noted down as the minimum shear strength and used in the statistical analyses. To determine sediment characteristics, we collected sediment samples with a gouge auger from 0 to 10, 10–20, 20–30, and 30–40 cm depth. Sometimes it was not possible to take sediment samples of all depths because of strongly compacted layers. At all measurement locations we also noted down present vegetation species.

We took erosion test samples at a selection of locations to measure erosion resistance under fast water flow (as may occur during a dike breach) in a flume, and from the same samples we determined belowground biomass. To study the effects of vegetation and inundation duration on erosion resistance, these samples were taken at the MR-site in tussock 1 (relatively short inundation duration) and on the bare mudflat next to it, as well as in tussock 2 (relatively long inundation duration) and on the bare mudflat next to it, at each location with four replicates. To study the effects of grain size, vegetation, and inundation duration on erosion resistance, we took these samples at the SN-site in section 5 % at the high marsh and bare mudflat, as well as in section 50 % at the high marsh and bare mudflat, also at each location with four replicates. We used a metal frame to take the erosion test samples of 40 cm long x 13 cm wide x 20 cm deep, according to the methodology described in Marin-Diaz et al. (2022). The samples were placed in boxes for transport and stored in saline water (30 PSU) to prevent them from drying out before the erosion tests. Transport did not visually result in additional sediment consolidation, which could potentially have affected sediment erosion resistance. Before testing the erosion resistance of these samples, 8 cm was cut off at one side of the samples to determine belowground biomass, leaving samples of 32 × 13 × 20 cm for the erosion test.

2.4. Laboratory measurements on sediment properties and belowground biomass

In the laboratory we weighed all wet sediment samples that were taken with the gouge auger, froze, and freeze-dried them, and weighed their dry weight afterwards. From these weights and their volume, water content and dry bulk density (herein referred to as bulk density) were calculated. We sieved the samples over a 1 mm sieve to remove large particles and belowground biomass, and then analyzed grain size distribution, including fine fraction content (clay + silt, < 63 μm), using a Mastersizer 2000 (Malvern Panalytical, UK).

The 8 × 13 × 20 cm samples that were cut off from the erosion test samples were sieved over a 3 mm sieve to extract belowground biomass. We placed the belowground biomass in a 60 °C oven for two weeks, and afterwards weighed dry biomass.

2.5. Flume measurements on erosion resistance

Sediment erosion resistance of the erosion test samples was measured in a fast flow flume, following the principles described by Marin-Diaz et al. (2022). For this study, a new, improved version of this flume was used (Appendix A: Fast flow flume, Fig. A.1). The new fast flow flume consists of three water tanks, each of which opens into four flow channels, through four openings of 11 cm wide x 2 cm high. Flow speed in the flow channels was 4.3 m s^{-1} (Appendix A: Fast flow flume). Such a high flow velocity simulates the flow conditions that can be reached over a tidal marsh after a dike breach under storm surge conditions (Albers, 2014; Kamrath et al., 2006).

The shoots of the erosion test samples were clipped to exclusively measure sediment erosion resistance without interference of aboveground biomass effects and the samples were placed in the flow channels. Each channel had two side panels to lock the samples in place, leaving a surface area of 32 cm long × 11 cm wide exposed to the water flow. At the start, after 10 min, and after 1, 2, and 3 h of water flow we measured the sediment surface level of the erosion test sample. These surface level measurements were done according to the sedimentation-erosion bar method (Nolte et al., 2013), where a bar with holes was laid over the sediment sample, always at the exact same location. A metal pin was lowered through the holes until it touched the sediment surface, after which the length of the pin above the bar was measured to determine the sediment surface level. The fixed positions of the holes ensured that the measurement points were always the same. The measurement points lay in two lines over the sample parallel to the water flow, 3 cm apart, and there were ten points per line, 3.7 cm apart (resulting in a total of 20 measurement points). To calculate erosion at each of the measurement moments, we subtracted the sediment surface levels after 10 min and 1, 2, and 3 h from the surface level at the start of the experiment. To quantify the erosion behaviour of the sediment samples in the fast flow flume, the erosion data were translated into a sediment loss rate (Appendix A: Fast flow flume).

2.6. Data and statistical analyses

All data and statistical analyses were performed in R, version 4.3.0 (R Core Team, 2023).

To correct bed elevation data for the different tidal ranges of the two studied marshes, we translated bed elevation data into tidal inundation duration data using water level data from Rijkswaterstaat Waterinfo (Rijkswaterstaat, 2023). We defined tidal inundation duration here as the percentage of time or hours per day a given location is submerged (Balke et al., 2016). We downloaded water level data from January 1st 2023 until December 31st 2023, recorded with a 10 min interval, for the closest tide gauge for both tidal marshes. These were Walsoorden for the MR-site and Delfzijl for the SN-site.

We used the dplyr package (Wickham et al., 2023) to calculate averages and standard deviations of the measured variables for all locations. We tested our data for normality with Shapiro-Wilk tests. If our data was normally distributed (only shear strength data of deeper layers at the SN-site and belowground biomass data of vegetated locations for the MR- and SN-sites combined), we applied ANOVA and Tukey HSD tests to test the significance of differences. Where this was not the case (all other data), we applied Kruskal-Wallis tests and Dunn's tests with Bonferroni correction for the *p*-values. We used linear regressions to study relationships between erosion, shear strength, inundation duration, sediment characteristics, and belowground biomass.

3. Results

3.1. Inundation duration, sediment grain size, and belowground biomass

Average inundation duration of all our measurement locations combined was significantly longer at the MR-site (38.9 ± 4.7 %) than at the SN-site (14.1 ± 8.7 %; $\chi^2 = 58$, $p < 0.001$; Fig. 2). At the MR-site, inundation duration did not significantly differ between the vegetated and bare locations ($\chi^2 = 0.98$, $p = 0.32$), but inundation duration between the tussocks did significantly differ ($\chi^2 = 41$, $p < 0.001$; Fig. 2a). A Dunn's test showed that inundation duration of tussocks 1 and 4 was significantly shorter than that of the other tussocks (e.g. $p = 0.002$ between tussocks 1 and 6 and $p < 0.001$ between tussocks 4 and 3). At the SN-site, inundation duration was not significantly different between the different sections for all locations combined ($\chi^2 = 4.8$, $p = 0.089$; Fig. 2b). However, when excluding the bare tidal flat locations (looking at only the high and mid marsh locations), section 5 % had the shortest inundation duration, followed by section 20 % and then by section 50 % ($\chi^2 = 20$, $p < 0.001$). Inundation duration of the high and mid marsh locations was significantly shorter than that of the bare tidal flat locations ($\chi^2 = 24$, $p < 0.001$; Fig. 2b).

Average median grain size was more than two times higher at the SN-site (118.0 ± 55.9 μm) than at the MR-site (41.3 ± 27.3 μm), and there was more variability in median grain size at the SN-site (Fig. 3). At the MR-site the median grain size of the top 10 cm of all vegetated locations did not significantly differ from that of all bare tidal flat locations ($\chi^2 = 0.58$, $p = 0.446$), but there were significant differences in median grain size between the tussocks ($\chi^2 = 39$, $p < 0.001$; Fig. 3a). Average median grain size of the top 10 cm at tussock 1 was much higher (99.2 ± 30.7 μm) than at the other five tussocks (ranging between 15.9 and 37.7 μm). At the SN-site median grain size of the top 10 cm was significantly higher in section 5 % than in sections 20 and 50 % ($\chi^2 = 15$, $p < 0.001$; Fig. 3b). There was no significant difference between sections 20 and 50 % ($p = 1.000$ in a Dunn's test), likely due to the enormous variability caused by the clay and silt being patchily distributed in the sandy matrix. The bare tidal flat locations had a higher median grain size of the top 10 cm than the high and mid marsh locations ($\chi^2 = 7.4$, $p = 0.024$). Most of the fine fraction content (clay + silt, < 63 μm) patterns were similar but in the opposite direction as those of median grain size (so high fine fraction content where median grain size was low, and vice versa; Appendix B: Fine fraction content and bulk density depth profiles, Fig. B.1).

Only *Spartina anglica* was present at the MR-site, and therefore all belowground biomass that we sampled there was of *Spartina anglica* as well. *Salicornia procumbens* and *Salicornia europaea* were the dominant species at the SN-site, but some other species occurred as well, such as *Puccinellia maritima*, *Suaeda maritima*, *Spergularia marina*, and *Aster tripolium*. Due to these species differences, the belowground biomass of the vegetated locations was significantly higher at the MR-site than at the SN-site ($F_{1,14} = 35$, $p < 0.001$), while belowground biomass of the bare locations was significantly higher at the SN-site than at the MR-site ($\chi^2 = 4.9$, $p = 0.027$; Fig. 4). At the SN-site it seemed like a relict root network was present in the samples of the bare tidal flat, likely resulting from the presence of vegetation in earlier years (e.g. in 2020; De Vries et al., 2021). At the MR-site the vegetated locations had significantly higher belowground biomass than the bare tidal flat locations where roots were absent ($\chi^2 = 13$, $p < 0.001$), while no significant difference existed between tussocks 1 and 2 ($\chi^2 = 0.81$, $p = 0.370$; Fig. 4a). At the SN-site the vegetated high marsh locations had significantly higher belowground biomass than the bare tidal flat locations ($\chi^2 = 6.4$, $p = 0.011$), and belowground biomass was higher in section 50 % than in section 5 % ($\chi^2 = 5.2$, $p = 0.023$; Fig. 4b).

3.2. Sediment strength and erosion resistance

Average surface shear strength of all locations combined was significantly higher at the SN-site (8.25 ± 3.87 kPa) than at the MR-site (1.11 ± 0.61 kPa; $\chi^2 = 61$, $p < 0.001$; Fig. 5). At the MR-site, overall

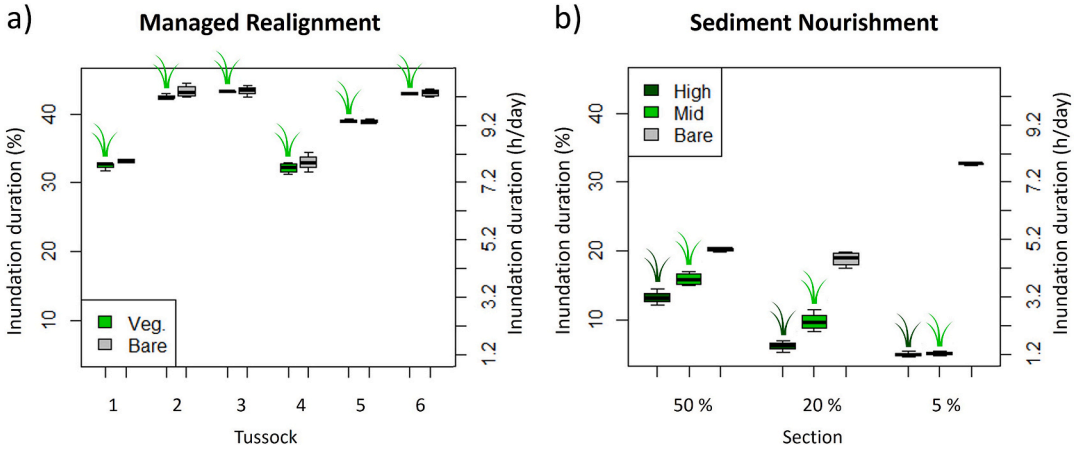

Fig. 2. Inundation duration of all measurement locations ($n = 4$) in % and average hours/day at the MR-site (a) and at the SN-site (b). Vegetation symbols above the boxplots indicate the vegetated locations. a) Light green indicates the vegetated locations inside the tussocks (Veg.) and grey the bare tidal flat locations next to the tussocks (Bare). b) Dark green indicates the high tidal marsh locations (High), light green the mid tidal marsh locations (Mid), and grey the bare tidal flat locations (Bare). (For interpretation of the references to colour in this figure legend, the reader is referred to the web version of this article.)

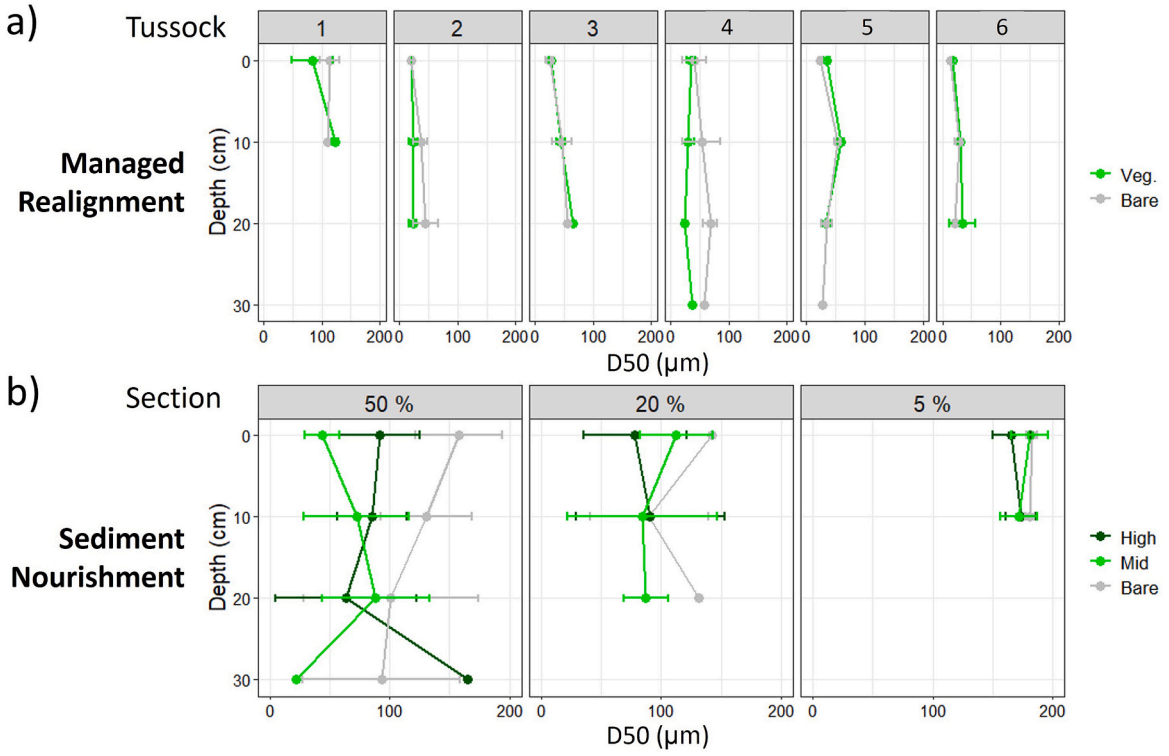

Fig. 3. Depth profiles of median grain size (D50) of all measurement locations (n = 4) at the MR-site (a) and at the SN-site (b). The error bars indicate standard deviations. a) Light green indicates the vegetated locations inside the tussocks (Veg.) and grey the bare tidal flat locations next to the tussocks (Bare). b) Dark green indicates the high tidal marsh locations (High), light green the mid tidal marsh locations (Mid), and grey the bare tidal flat locations (Bare). (For interpretation of the references to colour in this figure legend, the reader is referred to the web version of this article.)

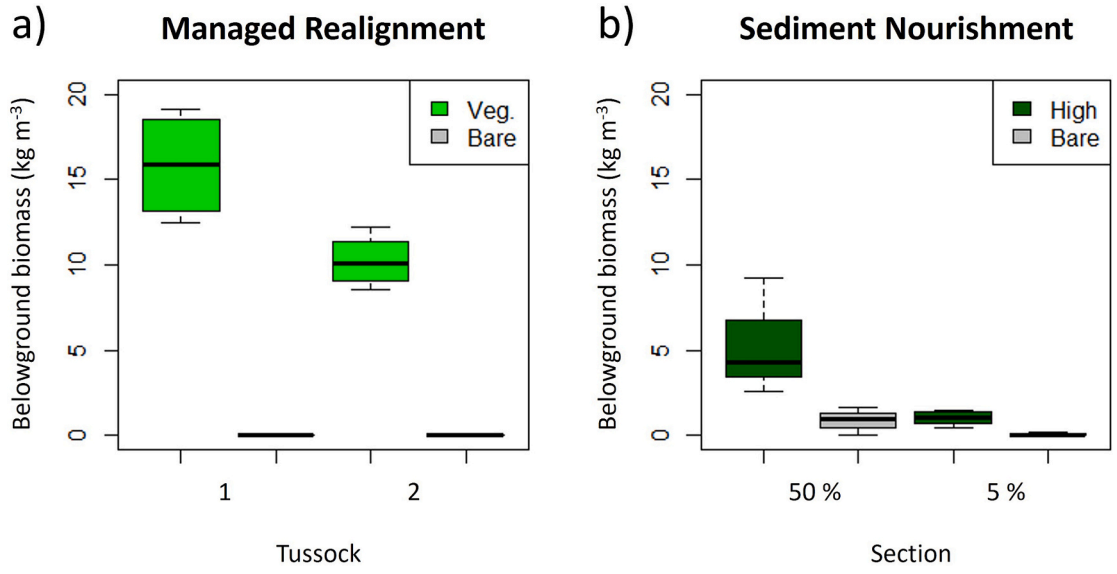

Fig. 4. Belowground biomass of a selection of locations (n = 4) at the MR-site (a) and at the SN-site (b). a) Light green indicates the vegetated locations inside the tussocks (Veg.) and grey the bare tidal flat locations next to the tussocks (Bare). b) Dark green indicates the high tidal marsh locations (High) and grey the bare tidal flat locations (Bare). (For interpretation of the references to colour in this figure legend, the reader is referred to the web version of this article.)

surface shear strength did not significantly differ between the vegetated and bare tidal flat locations ($\chi^2 = 2.6$, $p = 0.105$), but was significantly higher at tussocks 1 and 4 than at the other tussocks ($\chi^2 = 31$, $p < 0.001$; Fig. 5a). At the SN-site surface shear strength differed significantly between the three sections (highest in section 50 %, then in section 20 %, lowest in section 5 %; $\chi^2 = 8.2$, $p = 0.017$; Fig. 5b). In addition, surface shear strength was highest at the high marsh locations, followed by the mid marsh locations, and lowest at the bare tidal flat locations ($\chi^2 = 14$, $p < 0.001$).

At both the MR- and SN-site, shear strength generally increased with depth, but this was not always the case (.Fig. 6). At many of the tussocks of the MR-site we could not measure shear strength until 40 cm, since the shear vane was not able to penetrate the strongly compacted, relict agricultural soil, which was often present within 40 cm of the bed

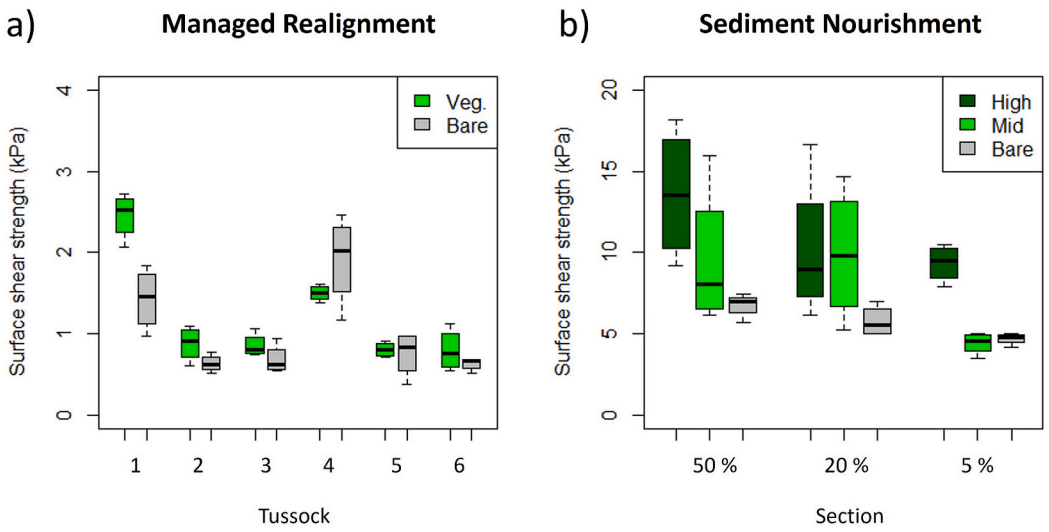

Fig. 5. Surface shear strength of all measurement locations (n = 4) at the MR-site (a) and at the SN-site (b). Please note that the y-axes of the MR- and SN-site are different. a) Light green indicates the vegetated locations inside the tussocks (Veg.) and grey the bare tidal flat locations next to the tussocks (Bare). b) Dark green indicates the high tidal marsh locations (High), light green the mid tidal marsh locations (Mid), and grey the bare tidal flat locations (Bare). (For interpretation of the references to colour in this figure legend, the reader is referred to the web version of this article.)

surface. At the MR-site shear strength at 10 cm depth was significantly higher within the vegetated tussocks than on the bare tidal flat ($\chi^2 = 4.2$, $p = 0.040$), although not for all tussocks separately (Fig. 6a). Significant differences in shear strength at 10 cm depth between tussocks existed ($\chi^2 = 26$, $p < 0.001$), and that of tussock 4 was the highest (Fig. 6a). At the SN-site shear strength at 10 cm depth was significantly higher at the vegetated high and mid marsh locations than at the bare tidal flat locations ($F_{2,33} = 5.5$, $p = 0.009$; Fig. 6b). In addition, section 20 % had the highest shear strength at 10 cm depth, followed by section 50 %, and section 5 % had the lowest ($F_{2,33} = 19$, $p < 0.001$; Fig. 6b).

The erosion test samples of both the MR- and SN-site had the highest erosion rates during the first 10 min of the erosion tests, after which they reduced more and more over the course of the flume runs (Fig. 7a, Fig. 7b). At the MR-site the samples of the bare mudflat locations had a

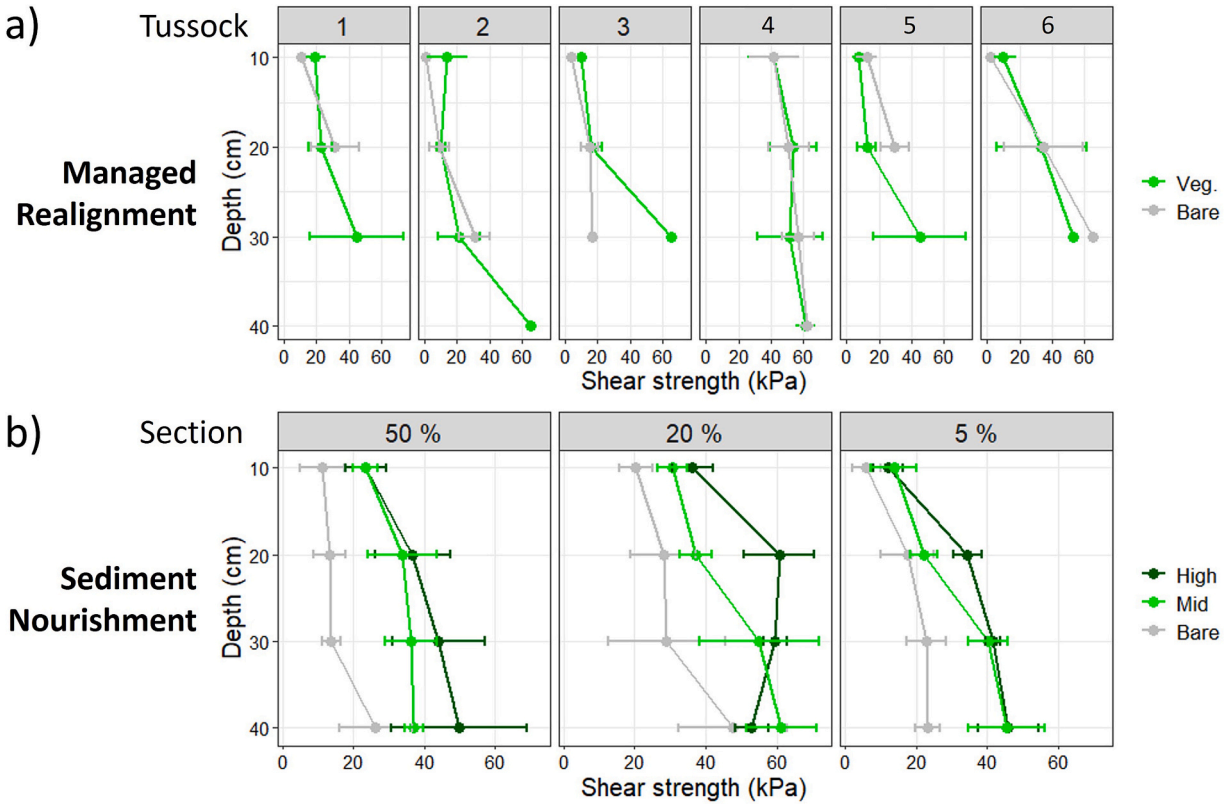

Fig. 6. Depth profiles of shear strength of all measurement locations (n = 4) at the MR-site (a) and at the SN-site (b). The error bars indicate standard deviations. a) Light green indicates the vegetated locations inside the tussocks (Veg.) and grey the bare tidal flat locations next to the tussocks (Bare). b) Dark green indicates the high tidal marsh locations (High), light green the mid tidal marsh locations (Mid), and grey the bare tidal flat locations (Bare). (For interpretation of the references to colour in this figure legend, the reader is referred to the web version of this article.)

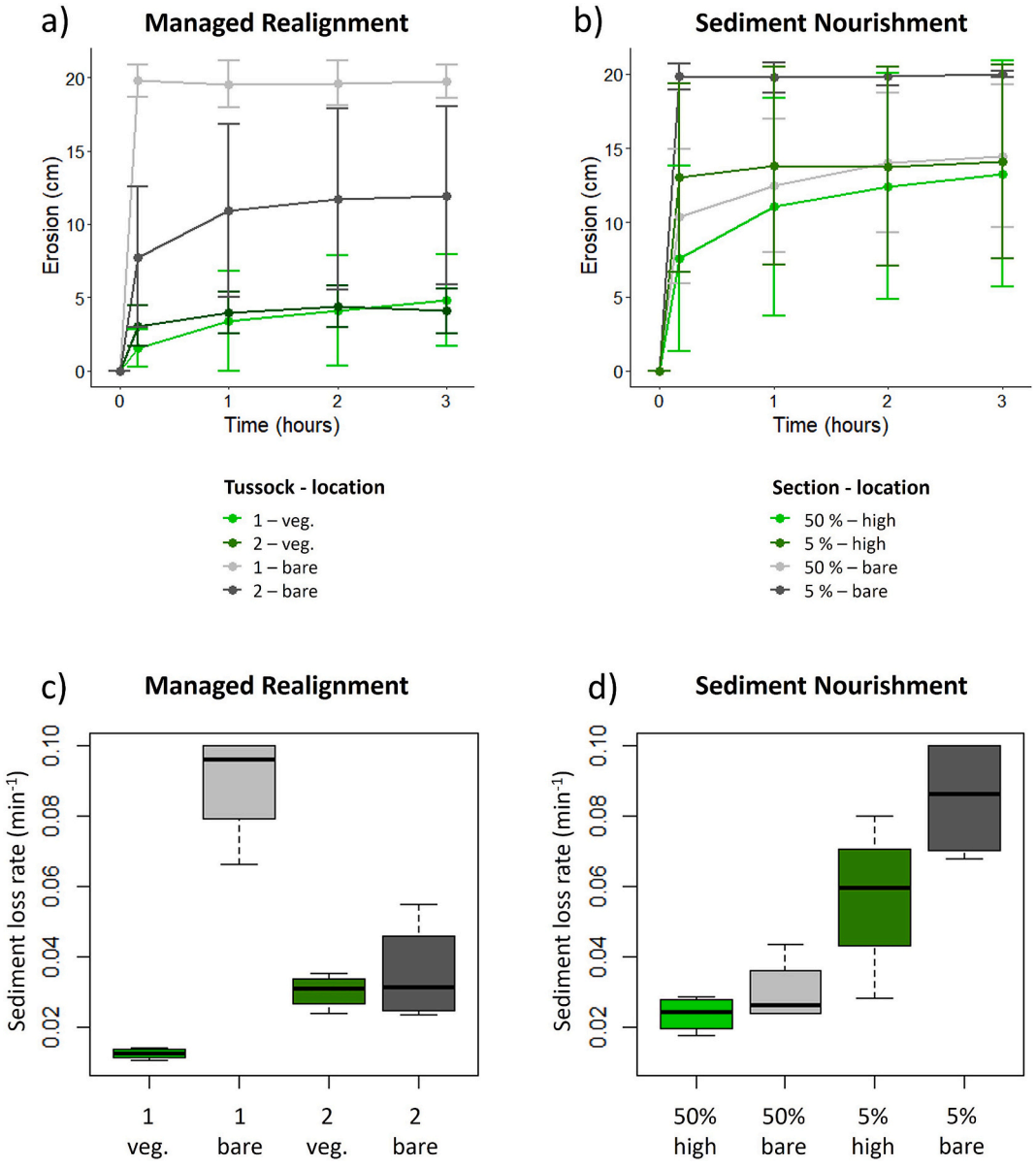

Fig. 7. a) Evolution of erosion of sediment samples from the MR-site over three hours in the fast flow flume. We measured erosion of vegetated locations within tussock 1 (light green), vegetated locations within tussock 2 (dark green), bare tidal flat locations close to tussock 1 (grey), and bare tidal flat locations close to tussock 2 (dark grey). Error bars indicate standard deviations. b) Evolution of erosion of sediment samples from the SN-site over three hours in the fast flow flume. We measured erosion of high marsh locations in section 50 % (light green), high marsh location in section 5 % (dark green), bare tidal flat locations in section 50 % (grey), and bare tidal flat locations in section 5 % (dark grey). Error bars indicate standard deviations. c) Sediment loss rates of the sampled locations at the MR-site (n = 4). Colors correspond to panel a. d) Sediment loss rates of the sampled locations at the SN-site (n = 4). Colors correspond to panel b. (For interpretation of the references to colour in this figure legend, the reader is referred to the web version of this article.)

significantly higher sediment loss rate than the samples of the vegetated locations within the tussocks ($\chi^2 = 6.9$, $p = 0.008$; Fig. 7c), so the bare mudflat location samples eroded faster. The loss rate did not differ between the two tussocks ($\chi^2 = 0$, $p = 1.000$; Fig. 7c), as especially the vegetated locations of the two tussocks eroded similarly (Fig. 7a). At the SN-site the sediment loss rate was higher in the samples of section 5 % than in the samples of section 50 %, ($\chi^2 = 9.3$, $p = 0.002$; Fig. 7d), indicating that the section 5 % samples eroded faster. The loss rates of the bare tidal flat and high marsh did not differ ($\chi^2 = 1.6$, $p = 0.207$). The samples of the bare tidal flat in section 5 % had fully eroded after 3 h, while the samples of the other locations had not (Fig. 7b). The vegetated samples of the MR-site had eroded significantly less after 3 h than those of the SN-site ($\chi^2 = 96$, $p < 0.001$; Fig. 7a, Fig. 7b), indicating that those of the MR-site were more erosion resistant.

3.3. Relationships between erosion, shear strength, inundation duration, sediment, and biomass

Many relationships existed at both sites between sediment loss rates, shear strength, inundation duration, sediment characteristics, and belowground biomass (Fig. 8). Shear strength at 10 cm depth decreased with increasing inundation duration at both sites (MR: $F_{1,46} = 37$, $R^2 = 0.44$, $p < 0.001$; SN: $F_{1,34} = 9.2$, $R^2 = 0.19$, $p = 0.005$), while surface shear strength only decreased with increasing inundation duration at the MR-site ($F_{1,46} = 77$, $R^2 = 0.62$, $p < 0.001$). At the MR-site, bulk density positively affected sediment loss rates ($F_{1,14} = 4.8$, $R^2 = 0.20$, $p = 0.047$), surface shear strength ($F_{1,46} = 33$, $R^2 = 0.40$, $p < 0.001$), and shear strength at 10 cm depth ($F_{1,46} = 17$, $R^2 = 0.25$, $p < 0.001$), while bulk density only positively affected sediment loss rates at the SN-site

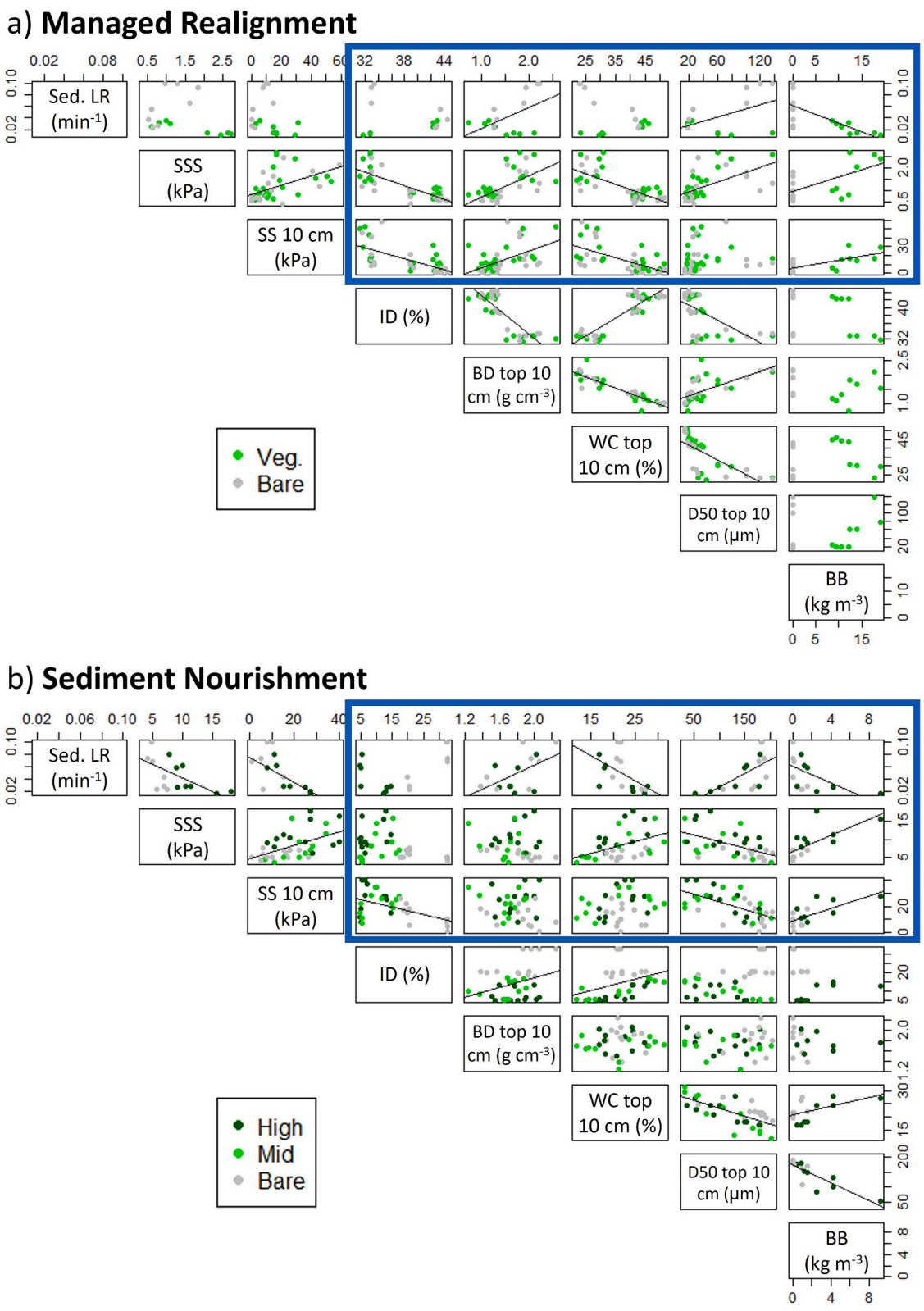

Fig. 8. Relationships between sediment loss rate (Sed. LR), surface shear strength (SSS), shear strength at 10 cm depth (SS 10 cm), inundation duration (ID), bulk density of the top 10 cm (BD top 10 cm), water content of the top 10 cm (WC top 10 cm), median grain size of the top 10 cm (D50 top 10 cm), and belowground biomass (BB) at the MR-site (a) and at the SN-site (b). A linear regression line indicates a significant ($p < 0.050$) correlation between two variables, the absence of a line a non-significant ($p > 0.050$) correlation. Relationships within the blue box are the key relationships that we studied here, the others might sometimes be auto-correlations (e.g. between bulk density and water content). a) Light green points indicate measurements at the vegetated locations inside the tussocks (Veg.) and grey points measurements at the bare tidal flat locations next to the tussocks (Bare). b) Dark green points indicate measurements at the high tidal marsh locations (High), light green points measurements at the mid tidal marsh locations (Mid), and grey points measurements at the bare tidal flat locations (Bare). (For interpretation of the references to colour in this figure legend, the reader is referred to the web version of this article.)

($F_{1,14} = 5.7$, $R^2 = 0.24$, $p = 0.032$). A negative relationship existed between water content and surface shear strength at the MR-site ($F_{1,46} = 58$, $R^2 = 0.55$, $p < 0.001$), while a positive one existed at the SN-site ($F_{1,34} = 7.6$, $R^2 = 0.16$, $p = 0.010$). Moreover, shear strength at 10 cm depth decreased with increasing water content at the MR-site ($F_{1,46} = 28$, $R^2 = 0.36$, $p < 0.001$), and sediment loss rates decreased with increasing water content at the SN-site ($F_{1,14} = 5.7$, $R^2 = 0.24$, $p = 0.031$). D50 positively affected sediment loss rates at both sites (MR: $F_{1,14} = 5.2$, $R^2 = 0.22$, $p = 0.038$; SN: $F_{1,14} = 10$, $R^2 = 0.37$, $p = 0.007$), and surface shear strength increased with increasing D50 at the MR-site ($F_{1,46} = 25$, $R^2 = 0.33$, $p < 0.001$). In contrast, shear strength at the surface and at 10 cm depth decreased with increasing D50 at the SN-site (surface: $F_{1,34} = 14$, $R^2 = 0.27$, $p < 0.001$; 10 cm depth: $F_{1,34} = 21$, $R^2 = 0.36$, $p < 0.001$). At both sites, negative relationships existed between belowground biomass and sediment loss rates (MR: $F_{1,14} = 13$, $R^2 = 0.44$, $p < 0.003$; SN: $F_{1,14} = 6.1$, $R^2 = 0.26$, $p = 0.027$), while belowground biomass positively affected shear strength at the surface (MR: $F_{1,14} = 8.3$, $R^2 = 0.33$, $p = 0.012$; SN: $F_{1,14} = 13$, $R^2 = 0.45$, $p = 0.003$) and at 10 cm depth (MR: $F_{1,14} = 13$, $R^2 = 0.45$, $p = 0.003$; SN: $F_{1,14} = 13$, $R^2 = 0.44$, $p = 0.003$). This indicates that the positive effects of belowground biomass on sediment strength and erosion resistance were most consistent, as well as the effects of bulk density and D50 on erosion resistance and the effect of inundation duration on shear strength at 10 cm depth. Many of the relationships that we found for the MR- and SN-site separately also existed when we combined the data of both sites (Appendix C: Relationships between erosion, shear strength, inundation duration, sediment, and biomass for the managed realignment and sediment nourishment marshes combined, Fig. C.1).

4. Discussion

This study showed that at both a managed realignment and sediment nourishment site sediment strength and erosion resistance were higher at vegetated locations than at unvegetated locations. In addition, at the managed realignment site – which is located low in the intertidal zone – inundation duration affected shear strength negatively, while bulk density affected shear strength positively. At the sediment nourishment site – which is built to a higher elevation in the intertidal zone suitable to host marsh vegetation – sediment grain size was the most important driving factor of shear strength and erosion resistance, besides vegetation presence: a decreasing shear strength and erosion resistance were observed with increasing sediment grain size.

4.1. Abiotic controls on the development of vegetation

Although previous literature found parabolic relationships between elevation and plant growth (Kirwan and Guntenspergen, 2012; Morris et al., 2002), we did not find significant relationships between inundation duration (which is a function of elevation, among others) and belowground biomass at either site (Fig. 8). The inundation duration range over which we measured may have been too small or other driving factors (such as grain size distribution) may have been dominant over inundation duration. Another possible explanation may be that morphological development and plant growth interact differently at restored and created tidal marshes than at natural tidal marshes due to the interventions that took place.

The significant higher belowground biomass that we found in section 50 % than in section 5 % at the SN-site (Fig. 4) may result from the higher levels of plant-available nutrients of fine sediments than sandy sediments (e.g. Staver et al., 2020). It has been shown that success in vegetation establishment and growth in sandy sediments can therefore be enhanced by the addition of fertilizer (Broome et al., 1988; Morris and Sundberg, 2024) or fine sediments (Delaune et al., 1990; Staver et al., 2020). Additionally, fine sediments generally have a higher water content than sandy sediments (Flemming and Delafontaine, 2000), which may speed up seed germination and vegetation establishment (Baptist et al., 2021; Doneen and Macgillivray, 1943; Noe and Zedler, 2000).

4.2. Abiotic controls on the development of sediment strength and erosion resistance

4.2.1. Inundation duration

Inundation duration of the MR-site was longer than that of the SN-site (Fig. 2), which is generally the case when applying managed realignment to low-lying, historically embanked land (van den Hoven et al., 2022). The former agricultural use of managed realignment sites generally leads to decades of soil subsidence, while tidal sediment supply and accretion are blocked by the protective dike, together leading to a bed surface elevation below mean sea level (Brunetta et al., 2019; Oosterlee et al., 2018; van den Hoven et al., 2022; Weisscher et al., 2022). At the SN-site, the bed surface elevation was artificially raised with sand enriched with a percentage of dredged fine fraction material, to create an environment with a suitable elevation within the tidal frame for vegetation establishment (De Vries et al., 2021).

At the MR-site, the locations with shortest inundation duration had the highest sediment shear strength (Fig. 8a). Shorter inundation durations allow the sediment to dry out further, which could enhance drying-induced consolidation and thereby sediment strength (Colosimo et al., 2023; Dong et al., 2020; Grabowski et al., 2011). However, erosion resistance of the sampled bare mudflat with shorter inundation duration (near tussock 1) was lower than that of the sampled bare mudflat with longer inundation duration (near tussock 2; Fig. 7c). The larger sediment grain size of tussock 1 than of tussock 2 (Fig. 3a), and thus lower cohesion (Brooks et al., 2021; Grabowski et al., 2011), is the likely cause for the higher erodibility of tussock 1. This difference highlights the variability of sediment erodibility even at a single site.

At the SN-site, shear strength at 10 cm depth increased with decreasing inundation duration (Fig. 8b). It seemed as if this effect was mainly caused by the relatively high shear strength of vegetated high and mid marsh locations (short inundation duration) on the one hand and by the relatively low shear strength of bare mudflat locations (long inundation duration) on the other hand. This could indicate that vegetation presence is a stronger driver of sediment strength than inundation duration. This strong positive effect of vegetation on sediment strength was not surprising and aligns with existing literature (Chen et al., 2012; Gyssels et al., 2005; Stoorvogel et al., 2024a). Although inundation duration of the vegetated high and mid marsh locations in section 50 % was longer than of sections 20 % and 5 %, surface shear strength of the vegetated high and mid marsh locations was highest in section 50 % (Fig. 2b; Fig. 5b). This contradicts existing knowledge that sediment strength increases with decreasing inundation duration as a result of stronger drying-induced consolidation (Colosimo et al., 2023; Dong et al., 2020). However, section 50 % had a higher fine fraction content and therefore higher sediment cohesion than the other sections (Grabowski et al., 2011; Houwing, 1999; Van Ledden et al., 2004), which presumably led to the higher sediment strength. The higher sediment cohesion of section 50 % than of section 5 % is likely also the reason for the higher erosion resistance of section 50 % (Fig. 7d). From these findings we can conclude that at the SN-site the sediment grain size distribution of the nourished sediment mixture in early phases of development is a dominant driver of sediment strength and erosion resistance development, which is more important than inundation duration. This is probably due to the effect of sediment grain size distribution on cohesive sediment strength, with the sand fraction being typically non-cohesive and the silt and clay fraction having a cohesive nature (Grabowski et al., 2011; Houwing, 1999; Van Ledden et al., 2004). Shear strength of deeper sediment layers was highest in section 20 % (Fig. 6b), which might indicate that this section had the optimal conditions of relatively high sediment cohesion (higher than section 5 %) but also a relatively short inundation duration (shorter than section 50 %).

4.2.2. Sediment type

At the MR-site, we found that bulk density positively affected shear strength (Fig. 8a), resulting from the denser degree of packing of sediment grains (Grabowski et al., 2011). However, bare sediment from near tussock 1 (with higher bulk density; Appendix B: Fine fraction content and bulk density depth profiles, Fig. B.2) eroded faster than from near tussock 2 (with lower bulk density; Appendix B: Fine fraction content and bulk density depth profiles, Fig. B.2; Fig. 7c). The relatively high bulk density near tussock 1 was likely caused by a larger sand fraction (Appendix B: Fine fraction content and bulk density depth profiles, Fig. B.1) instead of by more consolidation, leading to less cohesion and thereby to a lower erosion resistance (Brooks et al., 2021; Feagin et al., 2009; Ford et al., 2016; Lo et al., 2017).

At the SN-site, there were no relationships between bulk density and shear strength, while we found a strong negative effect of median grain size on shear strength and erosion resistance (Fig. 8b). The lack of relationships with bulk density at the SN-site seems to be caused by a general lack of differences in bulk density between the sections and locations (Appendix B: Fine fraction content and bulk density depth profiles, Fig. B.2). The sediment at the SN-site is a mixture of sand and dredged fine fraction material and we visually observed that the sediment was not everywhere well-mixed and very heterogeneous. This large small-scale spatial variability in sediment properties might explain the variability in our bulk density data. More sandy sediments led to a higher erodibility, due to a lack of sediment cohesion (Brooks et al., 2021; Feagin et al., 2009; Ford et al., 2016; Lo et al., 2017). Marsh restoration or creation using sediment nourishment are done with both clayey/silty (Cornwell et al., 2020; Kadiri et al., 2011) and sandy (Croft et al., 2006) sediments, depending on the source of the nourished sediment (Kadiri et al., 2011). The resulting effect of the nourished material on the sand, silt, and clay content of the marsh sediment will strongly influence sediment erosion resistance, as shown in this study, as well as other parameters such as primary production and carbon burial (Staver et al., 2020).

4.3. Biotic controls on the development of sediment strength and erosion resistance

At the MR-site, we did not find a strong effect of vegetation presence on shear strength (Fig. 5a; Fig. 6a), but we did find that erosion resistance was significantly higher in the vegetated tussocks than on the bare mudflat (Fig. 7c). This agrees with previous studies that showed the protective effect of plant roots on erosion resistance (Lo et al., 2017; Marin-Diaz et al., 2022; Wang et al., 2017). Plant roots increase substrate stability and thereby reduce sediment erodibility (Gyssels et al., 2005). The smaller spatial scale of the shear strength tests (e.g. with the field inspection shear vane tester 5.1 cm^2 at the MR-site and 3.1 cm^2 at the SN-site) than of the erosion tests (352 cm^2) might be the reason that we did not find a vegetation effect on shear strength, since there is a probability that vegetation roots were not sufficiently sampled with the shear strength tests. We found positive effects of belowground biomass on erosion resistance and shear strength (Fig. 8a), as more roots will lead to a stronger increase in substrate stability (Brooks et al., 2021).

At the SN-site, the vegetated high and mid marsh locations had a higher shear strength than the bare locations (Fig. 5b; Fig. 6b), suggesting that the presence of vegetation increases sediment strength. However, the bare locations also had a longer inundation duration than the vegetated locations (Fig. 2b), making it difficult to separate the effects of sediment consolidation and vegetation growth. Belowground biomass increased erosion resistance and shear strength (Fig. 8b), showing that at least part of the difference between bare and vegetated locations can be explained by vegetation growth.

At both the MR- and SN-site, vegetation reduced erosion more at the sandier locations than at the more clayey locations (Fig. 7c; Fig. 7d). This difference is in line with earlier findings by e.g. Evans et al. (2022), Feagin et al. (2009), Lo et al. (2017), and Schoutens et al. (2019). As previously argued by these authors, sediment at the clayey locations was already cohesive (and therefore relatively erosion resistant) by itself, which probably reduced the vegetation effect.

At both the MR- and SN-site, locations with coarser sediment (D50 > ± 100 μm) and without vegetation eroded very fast under high flow velocities (up to 20 cm erosion within 10 min; Fig. 7), which is in line with fast-flow erosion results of Marin-Diaz et al. (2022) for (semi-) natural sandy tidal flats. However, more cohesive sediments and vegetation decreased erodibility under both marsh restoration/creation techniques (Fig. 7). These effects were also found for (semi-)natural tidal flats and marshes by Marin-Diaz et al. (2022), although we found that the silty tidal flat samples did not always completely erode. Moreover, our cohesive, vegetated samples of both the MR- and SN-site had after three hours under fast flow eroded more (more than 2 cm) than the silty pioneer marsh samples of Marin-Diaz et al. (2022) (generally less than 2 cm), potentially because the vegetation and sediment at the MR- and SN-site were still relatively young (at most from 2015 and 2018, respectively).

4.4. The development of restored and created tidal marshes

The *Spartina anglica* tussocks at the MR-site grew very dense and created a lot of belowground biomass (Fig. 4), which contributed strongly to the erosion resistance of the sediment (Figs. 7c; 9). *Spartina anglica* can grow very well in muddy sediments such as in the MR-site (Huckle et al., 2000). However, there was still little vegetation at the MR-site; only a few patches were vegetated. This likely resulted from the too low bed elevation to start marsh development and from the fact that *Spartina anglica* is a slow-colonizing species (Schwarz et al., 2018). The large proportion of bare surface makes the overall area currently vulnerable to erosion (Fig. 9). Hydrodynamic forces at managed realignment sites are generally smaller than in natural marshes though, due to the wave-sheltered conditions (Weisscher et al., 2022), so sediment accretion will likely be fast if suspended sediment concentrations are high enough (Coleman et al., 2022; Oosterlee et al., 2020; Weisscher et al., 2022). Once conditions will be more suitable for vegetation establishment, vegetation expansion can go very fast (Fivash et al., 2023), depending on the dominant vegetation species (Schwarz et al., 2018).

The SN-site seemed a more established marsh than the MR-site even though it is 3 years younger, as a more consistent vegetation coverage (not just tussocks) and more diverse plant species composition were observed (the tussocks at the MR-site only consist of *Spartina anglica*; Fig. 9). The higher coverage and diversity likely resulted from the higher bed surface elevation at the SN-site due to the sediment nourishment, leading to shorter inundation duration and more Windows of Opportunity for vegetation establishment (Balke et al., 2014; Hu et al., 2015), and the fact that *Salicornia* spp. is a fast-colonizing species (Schwarz et al., 2018). However, the vegetation at the SN-site was much sparser than the *Spartina anglica* tussocks at the MR-site (Fig. 4), and therefore contributed less strongly to sediment erosion resistance (Fig. 7; Fig. 9). Sandier sediment (such as in some sections of the SN-site) is likely to be colonised by the annual *Salicornia* spp. with a shallow and sparse root system (Chirol et al., 2021), instead of by *Spartina anglica*, also at locations where *Salicornia procumbens* was not seeded (Bouma et al., 2013; Langlois et al., 2003). Moreover, sediment nourishments are generally made with sandy sediment, which leads to sediments that are more easily erodible (Lo et al., 2017; Marin-Diaz et al., 2022). Even after three more years (the age difference between the MR- and SN-site) of development, it is not expected that the sandy sediments will have acquired a similar erosion resistance as finer, cohesive sediments, since grain size seemed a dominant driver of erosion resistance. Mixing finer sediment through the sand matrix is needed to increase cohesion and erosion resistance but it has shown to be difficult to create a well-mixed sediment (Fig. 9). More studies and tests on this mixing process or on the use of cohesive sediments in Building with Nature projects (as e.g. done in a

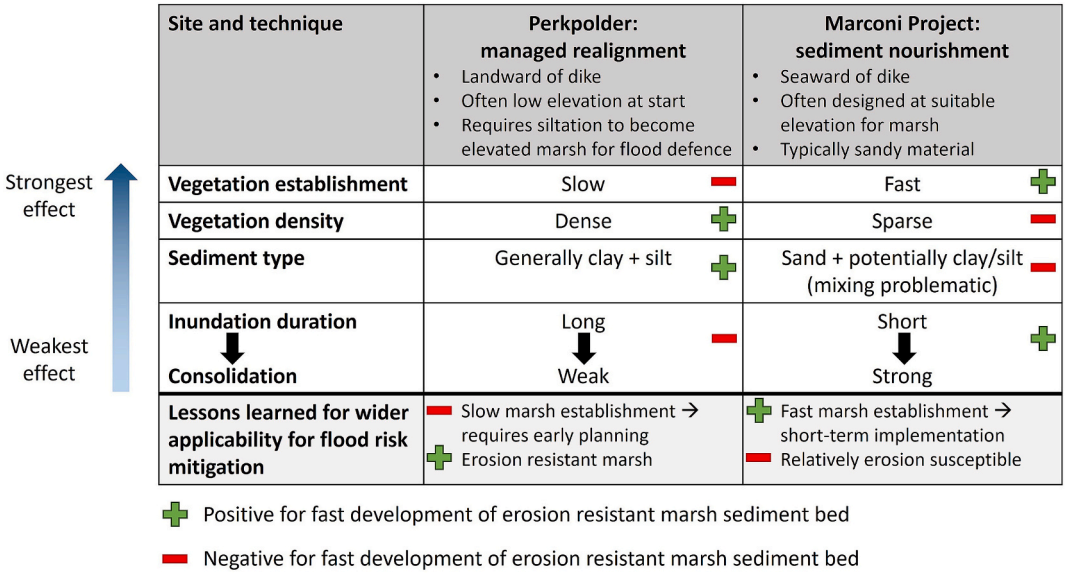

Fig. 9. Overview of the main factors that drive the development of erosion resistance at the managed realignment and sediment nourishment site studied here, and whether these affect a fast development of an erosion resistant marsh sediment bed for nature-based flood risk mitigation positively (green plus) or negatively (red minus). These conclusions are based on the comparison between two study sites. The arrow on the left indicates the strength of the driving factors. The lessons learned for the wider applicability of marshes for flood risk mitigation are shown in the bottom row, with green pluses indicating the positive effects and red minuses the negative effects on the applicability. (For interpretation of the references to colour in this figure legend, the reader is referred to the web version of this article.)

freshwater environment at the Marker Wadden, The Netherlands; Saaltink, 2018) could hopefully lead to insights in more successful techniques. In addition, the establishment of denser species with more biomass in such created marshes could be a solution that leads to a high vegetation coverage and strong increases in erosion resistance, offering good perspectives for using marshes created by sediment nourishment as part of nature-based flood risk mitigation.

4.5. Recommendations and conclusions for implementing marsh restoration and creation techniques to generate nature-based flood risk mitigation

Only two marsh restoration and creation sites were compared in this study, as the number of such existing sites is still relatively limited, which makes it difficult to make widely applicable recommendations for marsh restoration and creation to generate nature-based flood risk mitigation. However, this lack of sites makes it important to try to derive early lessons to enable larger-scale implementation. This study showed that tidal inundation duration, sediment characteristics, and vegetation presence and characteristics are all, although to a different extent, important factors driving the development of sediment strength and erosion resistance in tidal marsh restoration and creation projects (Fig. 9), which is in line with e.g. Evans et al. (2022), Ford et al. (2016), Lo et al. (2017), and Stoorvogel et al. (2024b). Therefore, if we want to apply marsh restoration and creation techniques, we should consider these factors to increase the marsh contribution to nature-based flood risk mitigation.

It is important to decide on the main goals of restoration or creation projects before their implementation. If we want to quickly create a fully established marsh with erosion resistant sediment for flood risk mitigation, it could be suitable to apply a sediment nourishment, but only if well-mixed with finer sediment (Fig. 9). If the mixing is successful, the combination of cohesive sediment and fast vegetation establishment (due to the suitable bed surface elevation) will lead to the fast development of an erosion resistant sediment bed. In addition, sediment nourishments will likely lead to a stronger contribution to flood risk mitigation through wave attenuation on the short-term than managed realignments, because of the faster development of a consistent vegetation coverage (Temmerman et al., 2023; Vuik et al., 2016). However, if the restoration or creation goals focus more on nature development, habitat creation and/or carbon sequestration, it might be more beneficial to let sediment naturally accrete (as in e.g. managed realignment), and thereby also stimulate tidal flat development (e.g. for bird foraging; Walles et al., 2019) and carbon sequestration (Temmink et al., 2022). If planned well ahead of time, natural accretion processes inherent to this approach will generate marshes that are erosion resistant (Fig. 9).

In conclusion, if the goal is to restore or create marshes for nature-based flood risk mitigation, we should decide what the most suitable restoration or creation technique is, depending on the specific location, goals, and available time. Moreover, we should consider the necessary bed surface elevation (affecting tidal inundation duration), vegetation establishment chances, expected vegetation species, and the envisioned sediment grain size, with the highest probability of leading to erosion resistant sediment beds. If we plan well ahead of time and temporarily support their development (with e.g. brushwood groynes), marshes have time to become erosion resistant, thereby preventing erosion shortly after the nature-based flood defence has been restored or created. This would enable sustainable use of marsh ecosystem services on the long-term.

Funding

This study is part of the project 'The Hedwige-Prosper Polder as a future-oriented experiment in managed realignment: integrating salt-marshes in water safety' (17589) of the research programme 'Living Labs in the Dutch Delta' which is funded by the Dutch Research Council (NWO) and co-funded by STOWA and EcoShape. Pim Willemsen was supported by the 'LIVING DIKES – Realising Resilient and Climate-Proof Coastal Protection' project of the NWA ORC research programme (NWA.1292.19.257) which is funded by the Dutch Research Council (NWO).

CRediT authorship contribution statement

Marte M. Stoorvogel: Writing – review & editing, Writing – original

draft, Visualization, Methodology, Investigation, Formal analysis, Conceptualization. **Pim W.J.M. Willemsen:** Writing – review & editing, Methodology, Conceptualization. **Jim van Belzen:** Writing – review & editing, Methodology, Conceptualization. **Stijn Temmerman:** Writing – review & editing, Supervision, Methodology, Funding acquisition, Conceptualization. **Jan M. de Jonge:** Writing – review & editing, Investigation. **Johan van de Koppel:** Writing – review & editing, Supervision, Methodology, Funding acquisition, Conceptualization. **Tjeerd J. Bouma:** Writing – review & editing, Supervision, Methodology, Funding acquisition, Conceptualization.

Declaration of competing interest

The authors declare that they have no known competing financial interests or personal relationships that could have appeared to influence the work reported in this paper.

Data availability

The data of this study are openly available in the research data repository 4TU: https://doi.org/10.4121/6ee17a0b-2d29-485c-9e1e-1f56648ddefc.

Acknowledgements

We thank all NIOZ colleagues and students who contributed to the fieldwork and laboratory measurements. We would like to thank Peter Herman for his valuable input on the study design. We are grateful for permission of Rijkswaterstaat to perform the measurements at Perkpolder, and of Gemeente Eemsdelta and Groningen Seaports to perform the measurements at Marconi. We thank Rijkswaterstaat for their publicly available water level data and aerial images. We would like to thank Lennart van IJzerloo and Zhenchang Zhu for planting and monitoring the vegetation tussocks at Perkpolder, and EcoShape for designing and monitoring Marconi. We would like to thank two reviewers for their feedback on our manuscript.

Appendix A. Fast flow flume

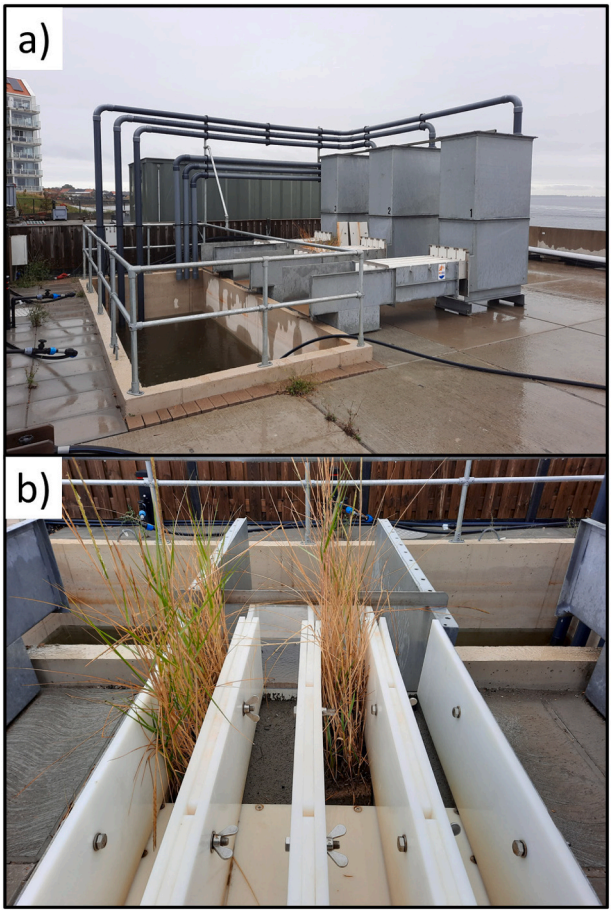

Fig. A.1. a) The fast flow flume with three vertical water tanks (on the right), and each water tank connects to four flow channels through four openings (11 cm wide x 2 cm high) at the bottom of the tank. Water is pumped from the water basin (on the left; 5.0 × 2.0 × 1.5 m) into the water tanks by three pumps (one for each tank). The water then flows from the water tanks through the flow channels over the sediment samples (one sample per flow channel) to test erosion resistance of the marsh sediment. The water flows from the flow channels back into the water basin. b) The sediment sample sections (40 × 13 × 22 cm) of four flow channels. Aboveground biomass was clipped before running the erosion test.

Flow velocity calculation for the fast flow flume

Flow velocity in the flow channel (u) of the fast flow flume was calculated, according to Van Rijn (1990), with

$$u = \frac{q}{h_2}$$

Where q is the discharge and h_2 is the minimum water depth behind the gate.
q was calculated with

$$q = h_0 h_2 \left(\frac{2g}{h_0 + h_2}\right)^{0.5}$$

Where h_0 is the water depth in the tank (0.945 m) and g is the gravitational acceleration (9.81 m s^{-2}).
h_2 was calculated with

$$h_2 = \mu\, h_1$$

Where μ is the contraction coefficient (0.6) and h_1 the height of the gate opening (0.02 m).

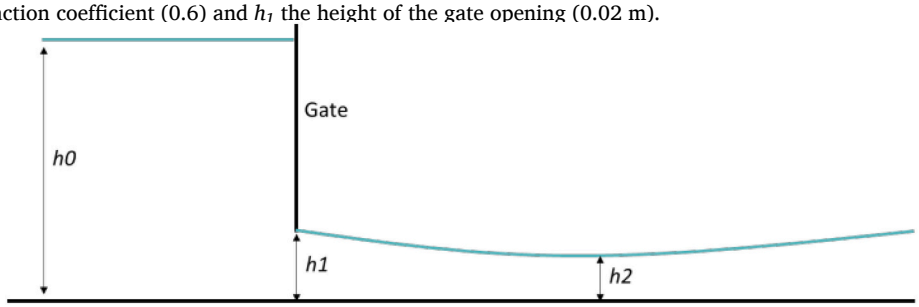

Fig. A.2. Flow in the fast flow flume channels under a gate and over a horizontal bottom (from Marin-Diaz et al., 2022).

Estimating sediment loss rates of erosion test samples

To quantify the erosion behaviour of the sediment samples in the fast flow flume, the erosion data were translated into a sediment loss rate. First, the average erosion was calculated (i.e. average vertical height change in mm) for each sample at every measurement moment (with $n = 20$). Then, we used the modified maximum likelihood estimator recently developed for survival analysis in continuous proportional data (Schotanus et al., 2020) to estimate the loss rate of the tested sediment samples due to erosion. We assumed that the loss (i.e. erosion) is proportional to the sediment volume present in the core and thus decays exponentially over time due to the applied supercritical flow regime. Therefore, the average lifetime τ of the sediment within the experiment was estimated following:

$$\tau = \frac{1}{1 - \rho_{t_{end}}} \sum_{i=1}^{n-1} ((1 - \rho_{i+1}) - (1 - \rho_i))t_{i+1}$$

Here ρ is the proportion of the total sediment retained at observation time t_i, n is the number of observations including the initial proportion at t_0. The estimated average experimental lifetime of the core was corrected for the uneroded proportion $\rho_{t_{end}}$ at the end of the flume run (i.e. censored observation).

Next, the rate at which the sediment sample was lost was determined by the decay constant ε, or loss rate. This loss rate ε is inversely related to the average lifetime τ of the sediment sample:

$$\varepsilon = \frac{1}{\tau}$$

Appendix B. Fine fraction content and bulk density depth profiles

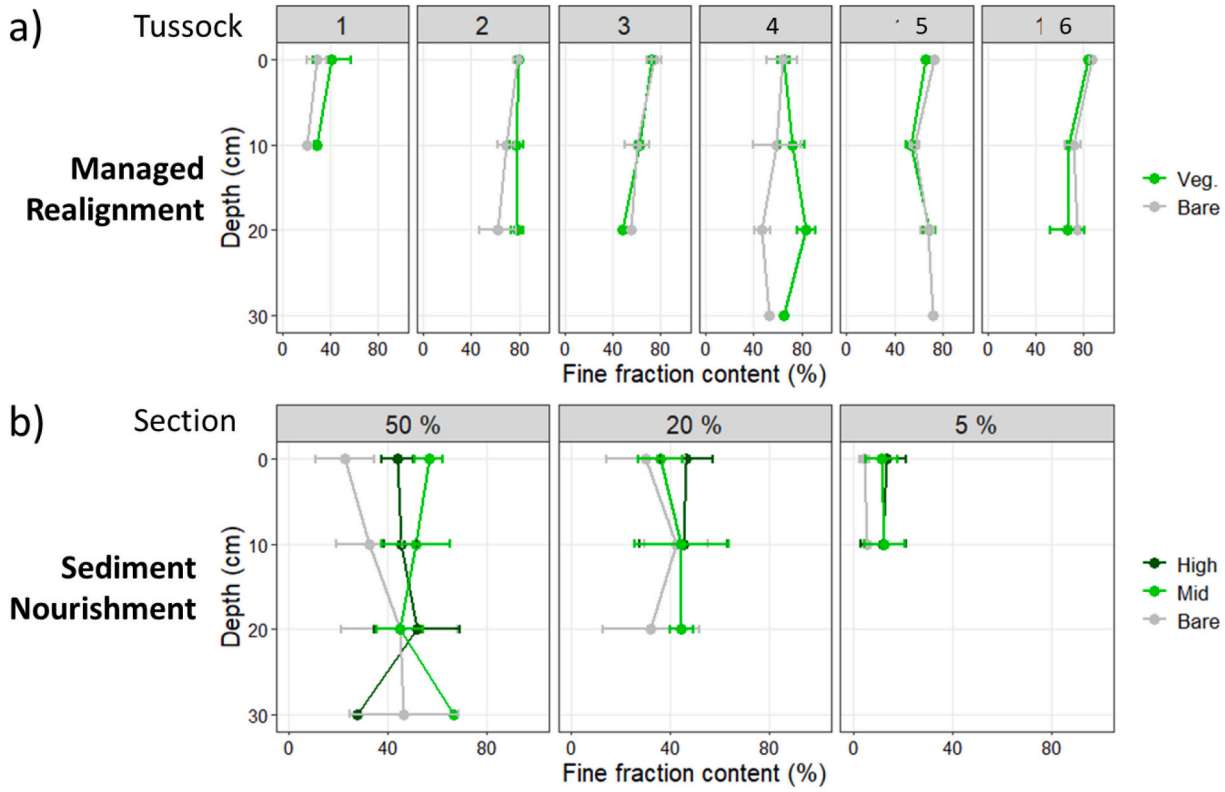

Fig. B.1. Depth profiles of fine fraction content (clay + silt, < 63 μm) of all measurement locations ($n = 4$) at the MR-site (a) and at the SN-site (b). The error bars indicate standard deviations. a) Light green indicates the vegetated locations inside the tussocks (Veg.) and grey the bare tidal flat locations next to the tussocks (Bare). b) Dark green indicates the high tidal marsh locations (High), light green the mid tidal marsh locations (Mid), and grey the bare tidal flat locations (Bare). (For interpretation of the references to colour in this figure legend, the reader is referred to the web version of this article.)

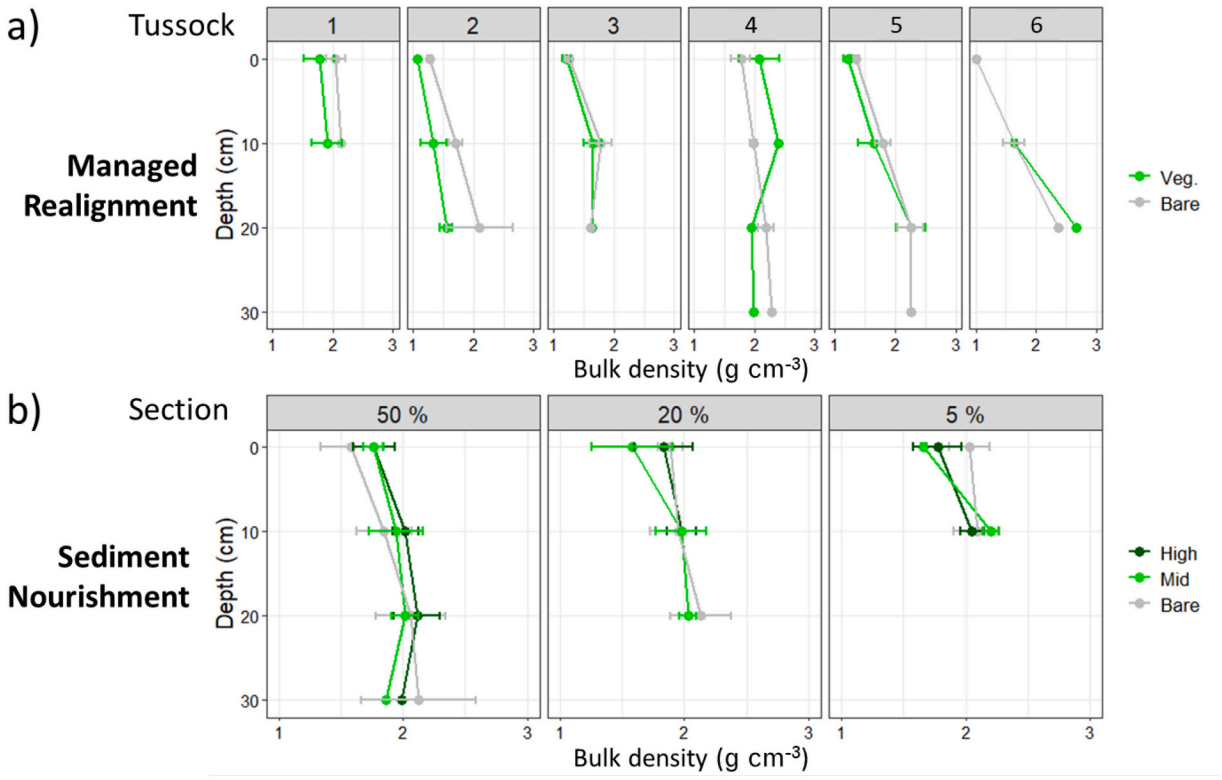

Fig. B.2. Depth profiles of bulk density of all measurement locations (n = 4) at the MR-site (a) and at the SN-site (b). The error bars indicate standard deviations. a) Light green indicates the vegetated locations inside the tussocks (Veg.) and grey the bare tidal flat locations next to the tussocks (Bare). b) Dark green indicates the high tidal marsh locations (High), light green the mid tidal marsh locations (Mid), and grey the bare tidal flat locations (Bare). (For interpretation of the references to colour in this figure legend, the reader is referred to the web version of this article.)

Appendix C. Relationships between erosion, shear strength, inundation duration, sediment, and biomass for the managed realignment and sediment nourishment marshes combined

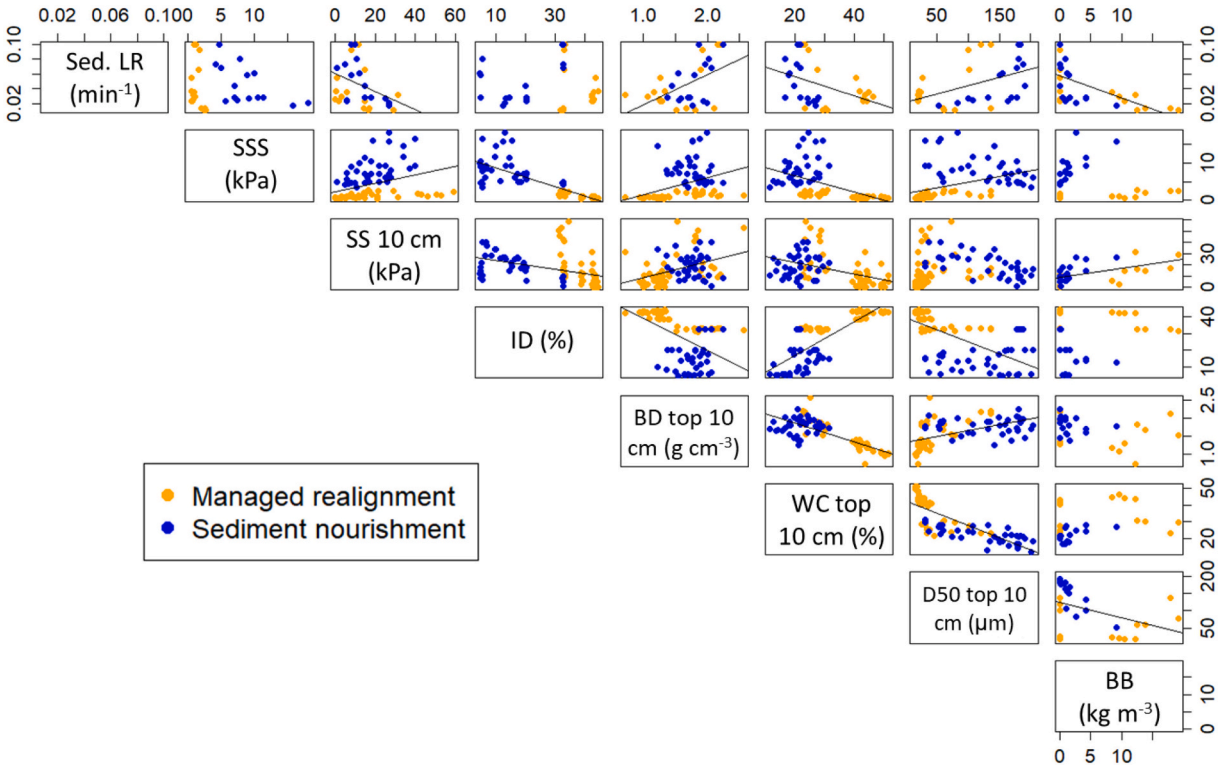

Fig. C.1. Relationships between sediment loss rate (Sed. LR), surface shear strength (SSS), shear strength at 10 cm depth (SS 10 cm), inundation duration (ID), bulk density of the top 10 cm (BD top 10 cm), water content of the top 10 cm (WC top 10 cm), median grain size of the top 10 cm (D50 top 10 cm), and belowground biomass (BB) at the MR-site (orange) and at the SN-site (blue). A linear regression line indicates a significant ($p < 0.050$) correlation between two variables, the absence of a line a non-significant correlation. (For interpretation of the references to colour in this figure legend, the reader is referred to the web version of this article.)

References

ABPmer, 2024. Coastal habitat creation scheme database. https://www.omreg.net/.

Albers, T.S., 2014. Emergency Closure of Dike Breaches: The Effect and Applicability of Emergency Measures. Delft University of Technology.

Balke, T., Herman, P.M.J., Bouma, T.J., 2014. Critical transitions in disturbance-driven ecosystems: Identifying windows of opportunity for recovery. J. Ecol. 102 (3), 700–708. https://doi.org/10.1111/1365-2745.12241.

Balke, T., Stock, M., Jensen, K., Bouma, T.J., Kleyer, M., 2016. A global analysis of the seaward salt marsh extent: the importance of tidal range. Water Resour. Res. 52 (5), 3775–3786. https://doi.org/10.1002/2015WR018318.

Baptist, M.J., Dankers, P., Cleveringa, J., Sittoni, L., Willemsen, P.W.J.M., van Puijenbroek, M.E.B., de Vries, B.M.L., Leuven, J.R.F.W., Coumou, L., Kramer, H., Elschot, K., 2021. Salt marsh construction as a nature-based solution in an estuarine social-ecological system. Nat. Based Sol. 1, 100005. https://doi.org/10.1016/j.nbsj.2021.100005.

Barbier, E.B., Hacker, S.D., Kennedy, C., Koch, E.W., Stier, A.C., Silliman, B.R., 2011. The value of estuarine and coastal ecosystem services. Ecol. Monogr. 81 (2), 169–193. https://doi.org/10.1890/10-1510.1.

Barciela-Rial, M., van Paassen, L.A., Griffioen, J., van Kessel, T., Winterwerp, J.C., 2020. The effect of solid-phase composition on the drying behavior of Markermeer sediment. Vadose Zone J. 19 (1), e20028. https://doi.org/10.1002/vzj2.20028.

Bouma, T.J., Temmerman, S., van Duren, L.A., Martini, E., Vandenbruwaene, W., Callaghan, D.P., Balke, T., Biermans, G., Klaassen, P.C., van Steeg, P., Dekker, F., van de Koppel, J., de Vries, M.B., Herman, P.M.J., 2013. Organism traits determine the strength of scale-dependent bio-geomorphic feedbacks: a flume study on three intertidal plant species. Geomorphology 180–181, 57–65. https://doi.org/10.1016/j.geomorph.2012.09.005.

Brooks, H., Möller, I., Carr, S., Chirol, C., Christie, E., Evans, B., Spencer, K.L., Spencer, T., Royse, K., 2021. Resistance of salt marsh substrates to near-instantaneous hydrodynamic forcing. Earth Surf. Process. Landf. 46 (1), 67–88. https://doi.org/10.1002/esp.4912.

Broome, S.W., Seneca, E.D., Woodhouse, W.W., 1988. Tidal salt marsh restoration. Aquat. Bot. 32, 1–22. https://doi.org/10.1016/0304-3770(88)90085-X.

Brunetta, R., de Paiva, J.S., Ciavola, P., 2019. Morphological evolution of an intertidal area following a set-back scheme: a case study from the Perkpolder Basin (Netherlands). Front. Earth Sci. 7, 228. https://doi.org/10.3389/feart.2019.00228.

Chen, Y., Thompson, C.E.L., Collins, M.B., 2012. Saltmarsh creek bank stability: biostabilisation and consolidation with depth. Cont. Shelf Res. 35, 64–74. https://doi.org/10.1016/j.csr.2011.12.009.

Chirol, C., Spencer, K.L., Carr, S.J., Möller, I., Evans, B., Lynch, J., Brooks, H., Royse, K. R., 2021. Effect of vegetation cover and sediment type on 3D subsurface structure and shear strength in saltmarshes. Earth Surf. Process. Landf. 46 (11), 2279–2297. https://doi.org/10.1002/esp.5174.

Coleman, D.J., Schuerch, M., Temmerman, S., Guntenspergen, G., Smith, C.G., Kirwan, M.L., 2022. Reconciling models and measurements of marsh vulnerability to sea level rise. Limnol. Oceanogr. Lett. 7 (2), 140–149. https://doi.org/10.1002/lol2.10230.

Colosimo, I., van Maren, D.S., de Vet, P.L.M., Winterwerp, J.C., van Prooijen, B.C., 2023. Winds of opportunity: the effects of wind on intertidal flat accretion. Geomorphology 108840. https://doi.org/10.1016/j.geomorph.2023.108840.

Cornwell, J.C., Owens, M.S., Staver, L.W., Stevenson, J.C., 2020. Tidal marsh restoration at Poplar Island I: transformation of estuarine sediments into marsh soils. Wetlands 40, 1673–1686. https://doi.org/10.1007/s13157-020-01294-5/Published.

Croft, A.L., Leonard, L.A., Alphin, T.D., Cahoon, L.B., Posey, M.H., 2006. The effects of thin layer sand renourishment on tidal marsh processes: Masonboro Island, North Carolina. Estuar. Coasts 29 (5), 737–750. https://doi.org/10.1007/BF02786525.

De Groot, A.V., Van Duin, W.E., 2013. Best Practices for Creating New Salt Marshes in an Estuarine Setting, a Literature Study. IMARES, IJmuiden. https://edepot.wur.nl/248715.

De Vries, B., Willemsen, P., Van Puijenbroek, M.E.B., Coumou, L., Baptist, M.J., Cleveringa, J., Dankers, P., Elschot, K., 2021. Salt Marsh Pilot Marconi: Monitoring Results. EcoShape, Amersfoort.

Delaune, R.D., Pezeshki, S.R., Pardue, J.H., Whitcomb, J.H., Patrick, W.H., 1990. Some influences of sediment addition to a deteriorating salt marsh in the Mississippi River Deltaic plain: a pilot study. J. Coast. Res. 6 (1), 181–188.

Dijkema, K.S., Van Duin, W.E., Dijkman, E.M., Van Leeuwen, P.W., 2007. Monitoring van kwelders in de Waddenzee: Rapport in het kader van het WOT programma Informatievoorziening Natuur i.o. (WOT IN). Alterra, Wageningen.

Doneen, L.D., Macgillivray, J.H., 1943. Germination (emergence) of vegetable seed as affected by different soil moisture conditions. Plant Physiol. 18 (3), 524–529. https://doi.org/10.1104/pp.18.3.524.
Dong, Y., Lu, N., Fox, P.J., 2020. Drying-induced consolidation in soil. J. Geotech. Geoenviron. Eng. 146 (9), 04020092. https://doi.org/10.1061/(asce)gt.1943-5606.0002327.
Doody, J.P., 2013. Coastal squeeze and managed realignment in Southeast England, does it tell us anything about the future? Ocean Coast. Manag. 79, 34–41. https://doi.org/10.1016/j.ocecoaman.2012.05.008.
Duarte, C.M., Losada, I.J., Hendriks, I.E., Mazarrasa, I., Marbà, N., 2013. The role of coastal plant communities for climate change mitigation and adaptation. Nat. Clim. Chang. 3 (11), 961–968. https://doi.org/10.1038/nclimate1970.
Eems-Dollard 2050, n.d. Marconi Buitendijks. Retrieved January 29, 2024, from https://eemsdollard2050.nl/project/marconi/.
Evans, B.R., Brooks, H., Chirol, C., Kirkham, M.K., Möller, I., Royse, K., Spencer, K., Spencer, T., 2022. Vegetation interactions with geotechnical properties and erodibility of salt marsh sediments. Estuar. Coast. Shelf Sci. 265, 107713. https://doi.org/10.1016/j.ecss.2021.107713.
Fagherazzi, S., Kirwan, M.L., Mudd, S.M., Guntenspergen, G.R., Temmerman, S., D'Alpaos, A., Van De Koppel, J., Rybczyk, J.M., Reyes, E., Craft, C., Clough, J., 2012. Numerical models of salt marsh evolution: ecological, geomorphic, and climatic factors. Rev. Geophys. 50 (1), RG1002. https://doi.org/10.1029/2011RG000359.
Fairchild, T.P., Bennett, W.G., Smith, G., Day, B., Skov, M.W., Möller, I., Beaumont, N., Karunarathna, H., Griffin, J.N., 2021. Coastal wetlands mitigate storm flooding and associated costs in estuaries. Environ. Res. Lett. 16 (7). https://doi.org/10.1088/1748-9326/ac0c45.
Feagin, R.A., Lozada-Bernard, S.M., Ravens, T.M., Möller, I., Yeager, K.M., Baird, A.H., 2009. Does vegetation prevent wave erosion of salt marsh edges? Proc. Natl. Acad. Sci. USA 106 (25), 10109–10113. https://doi.org/10.1073/pnas.0901297106.
Fivash, G.S., Temmerman, S., Kleinhans, M.G., Heuner, M., van der Heide, T., Bouma, T. J., 2023. Early indicators of tidal ecosystem shifts in estuaries. Nat. Commun. 14 (1), 1911. https://doi.org/10.1038/s41467-023-37444-6.
Flemming, B.W., Delafontaine, M.T., 2000. Mass physical properties of muddy intertidal sediments: some applications, misapplications and non-applications. Cont. Shelf Res. 20, 1179–1197. https://doi.org/10.1016/S0278-4343(00)00018-2.
Ford, H., Garbutt, A., Ladd, C., Malarkey, J., Skov, M.W., 2016. Soil stabilization linked to plant diversity and environmental context in coastal wetlands. J. Veg. Sci. 27 (2), 259–268. https://doi.org/10.1111/jvs.12367.
French, P.W., 2006. Managed realignment - the developing story of a comparatively new approach to soft engineering. Estuar. Coast. Shelf Sci. 67 (3), 409–423. https://doi.org/10.1016/j.ecss.2005.11.035.
Gedan, K.B., Kirwan, M.L., Wolanski, E., Barbier, E.B., Silliman, B.R., 2011. The present and future role of coastal wetland vegetation in protecting shorelines: answering recent challenges to the paradigm. Clim. Chang. 106 (1), 7–29. https://doi.org/10.1007/s10584-010-0003-7.
Gemeente Eemsdelta, n.d. Marconi Buitendijks. Retrieved January 29, 2024, from https://eemsdelta.nl/marconi-buitendijks.
Gourgue, O., Van Belzen, J., Schwarz, C., Vandenbruwaene, W., Vanlede, J., Belliard, J. P., Fagherazzi, S., Bouma, T.J., Van De Koppel, J., Temmerman, S., 2022. Biogeomorphic modeling to assess the resilience of tidal-marsh restoration to sea level rise and sediment supply. Earth Surf. Dyn. 10 (3), 531–553. https://doi.org/10.5194/esurf-10-531-2022.
Grabowski, R.C., Droppo, I.G., Wharton, G., 2011. Erodibility of cohesive sediment: the importance of sediment properties. Earth Sci. Rev. 105 (3–4), 101–120. https://doi.org/10.1016/j.earscirev.2011.01.008.
Gyssels, G., Poesen, J., Bochet, E., Li, Y., 2005. Impact of plant roots on the resistance of soils to erosion by water: a review. Prog. Phys. Geogr. 29 (2), 189–217. https://doi.org/10.1191/0309133305pp443ra.
Houwing, E.-J., 1999. Determination of the critical erosion threshold of cohesive sediments on intertidal mudflats along the Dutch Wadden Sea Coast. Estuar. Coast. Shelf Sci. 49, 545–555. https://doi.org/10.1006/ecss.1999.0518.
Hu, Z., Van Belzen, J., Van Der Wal, D., Balke, T., Wang, Z.B., Stive, M., Bouma, T.J., 2015. Windows of opportunity for salt marsh vegetation establishment on bare tidal flats: the importance of temporal and spatial variability in hydrodynamic forcing. J. Geophys. Res. G Biogeosci. 120 (7), 1450–1469. https://doi.org/10.1002/2014JG002870.
Huckle, J.M., Potter, J.A., Marrs, R.H., 2000. Influence of environmental factors on the growth and interactions between salt marsh plants: effects of salinity, sediment and waterlogging. J. Ecol. 88 (3), 492–505. https://doi.org/10.1046/j.1365-2745.2000.00464.x.
Kadiri, M., Spencer, K.L., Heppell, C.M., Fletcher, P., 2011. Sediment characteristics of a restored saltmarsh and mudflat in a managed realignment scheme in Southeast England. Hydrobiologia 672 (1), 79–89. https://doi.org/10.1007/s10750-011-0755-8.
Kamrath, P., Disse, M., Hammer, M., Köngeter, J., 2006. Assessment of discharge through a dike breach and simulation of flood wave propagation. Nat. Hazards 38 (1–2), 63–78. https://doi.org/10.1007/s11069-005-8600-x.
Kirwan, M.L., Guntenspergen, G.R., 2012. Feedbacks between inundation, root production, and shoot growth in a rapidly submerging brackish marsh. J. Ecol. 100 (3), 764–770. https://doi.org/10.1111/j.1365-2745.2012.01957.x.
Kirwan, M.L., Megonigal, J.P., 2013. Tidal wetland stability in the face of human impacts and sea-level rise. Nature 504 (7478), 53–60. https://doi.org/10.1038/nature12856.
Langlois, E., Bonis, A., Bouzillé, J.B., 2003. Sediment and plant dynamics in saltmarshes pioneer zone: Puccinellia maritima as a key species? Estuar. Coast. Shelf Sci. 56 (2), 239–249. https://doi.org/10.1016/S0272-7714(02)00185-3.
Lo, V.B., Bouma, T.J., van Belzen, J., Van Colen, C., Airoldi, L., 2017. Interactive effects of vegetation and sediment properties on erosion of salt marshes in the Northern Adriatic Sea. Mar. Environ. Res. 131, 32–42. https://doi.org/10.1016/j.marenvres.2017.09.006.
Marin-Diaz, B., Govers, L.L., van der Wal, D., Olff, H., Bouma, T.J., 2022. The importance of marshes providing soil stabilization to resist fast-flow erosion in case of a dike breach. Ecol. Appl. 32 (6), e2622. https://doi.org/10.1002/eap.2622.
Marin-Diaz, B., van der Wal, D., Kaptein, L., Martinez-Garcia, P., Lashley, C.H., de Jong, K., Nieuwenhuis, J.W., Govers, L.L., Olff, H., Bouma, T.J., 2023. Using salt marshes for coastal protection: effective but hard to get where needed most. J. Appl. Ecol. 60 (7), 1286–1301. https://doi.org/10.1111/1365-2664.14413.
Maris, T., Cox, T., Temmerman, S., De Vleeschauwer, P., Van Damme, S., De Mulder, T., Van Den Bergh, E., Meire, P., 2007. Tuning the tide: creating ecological conditions for tidal marsh development in a flood control area. Hydrobiologia 588 (1), 31–43. https://doi.org/10.1007/s10750-007-0650-5.
Möller, I., Kudella, M., Rupprecht, F., Spencer, T., Paul, M., Van Wesenbeeck, B.K., Wolters, G., Jensen, K., Bouma, T.J., Miranda-Lange, M., Schimmels, S., 2014. Wave attenuation over coastal salt marshes under storm surge conditions. Nat. Geosci. 7 (10), 727–731. https://doi.org/10.1038/NGEO2251.
Morris, J.T., Sundberg, K., 2024. Responses of coastal wetlands to rising sea-level revisited: the importance of organic production. Estuar. Coasts 47, 1735–1749. https://doi.org/10.1007/s12237-023-01313-8.
Morris, J.T., Sundareshwar, P.V., Nietch, C.T., Kjerfve, B., Cahoon, D.R., 2002. Responses of coastal wetlands to rising sea level. Ecology 83 (10), 2869–2877. https://doi.org/10.1890/0012-9658(2002)083[2869:ROCWTR]2.0.CO;2.
Nelson, J.L., Zavaleta, E.S., 2012. Salt marsh as a coastal filter for the oceans: changes in function with experimental increases in Nitrogen loading and sea-level rise. PLoS One 7 (8), e38558. https://doi.org/10.1371/journal.pone.0038558.
Noe, G.B., Zedler, J.B., 2000. Differential effects of four abiotic factors on the germination of salt marsh annuals. Am. J. Bot. 87 (11), 1679–1692. https://doi.org/10.2307/2656745.
Nolte, S., Koppenaal, E.C., Esselink, P., Dijkema, K.S., Schuerch, M., De Groot, A.V., Bakker, J.P., Temmerman, S., 2013. Measuring sedimentation in tidal marshes: a review on methods and their applicability in biogeomorphological studies. J. Coast. Conserv. 17 (3), 301–325. https://doi.org/10.1007/s11852-013-0238-3.
Oosterlee, L., Cox, T.J.S., Vandenbruwaene, W., Maris, T., Temmerman, S., Meire, P., 2018. Tidal marsh restoration design affects feedbacks between inundation and elevation change. Estuar. Coasts 41 (3), 613–625. https://doi.org/10.1007/s12237-017-0314-2.
Oosterlee, L., Cox, T.J.S., Temmerman, S., Meire, P., 2020. Effects of tidal re-introduction design on sedimentation rates in previously embanked tidal marshes. Estuar. Coast. Shelf Sci. 244, 106428. https://doi.org/10.1016/j.ecss.2019.106428.
R core team, 2023. R: A Language and Environment for Statistical Computing. R foundation for Statistical computing, Vienna, Austria. https://www.R-project.org/.
Rijkswaterstaat, 2023. Waterinfo. https://waterinfo.rws.nl/#!/nav/bulkdownload/huidige-selectie/.
Rogers, K., Kelleway, J.J., Saintilan, N., Megonigal, J.P., Adams, J.B., Holmquist, J.R., Lu, M., Schile-Beers, L., Zawadzki, A., Mazumder, D., Woodroffe, C.D., 2019. Wetland carbon storage controlled by millennial-scale variation in relative sea-level rise. Nature 567 (7746), 91–95. https://doi.org/10.1038/s41586-019-0951-7.
Saaltink, R.M., 2018. Wetland Eco-Engineering with Fine Sediment (Doctoral dissertation,. Utrecht University.
Schotanus, J., Walles, B., Capelle, J.J., van Belzen, J., van de Koppel, J., Bouma, T.J., 2020. Promoting self-facilitating feedback processes in coastal ecosystem engineers to increase restoration success: testing engineering measures. J. Appl. Ecol. 57 (10), 1958–1968. https://doi.org/10.1111/1365-2664.13709.
Schoutens, K., Heuner, M., Minden, V., Schulte Ostermann, T., Silinski, A., Belliard, J.P., Temmerman, S., 2019. How effective are tidal marshes as nature-based shoreline protection throughout seasons? Limnol. Oceanogr. 64 (4), 1750–1762. https://doi.org/10.1002/lno.11149.
Schoutens, K., Stoorvogel, M., van den Berg, M., van den Hoven, K., Bouma, T.J., Aarninkhof, S., Herman, P.M.J., van Loon-Steensma, J.M., Meire, P., Schoelynck, J., Peeters, P., Temmerman, S., 2022. Stability of a tidal marsh under very high flow velocities and implications for nature-based flood defense. Front. Mar. Sci. 9, 920480. https://doi.org/10.3389/fmars.2022.920480.
Schwarz, C., Gourgue, O., van Belzen, J., Zhu, Z., Bouma, T.J., van de Koppel, J., Ruessink, G., Claude, N., Temmerman, S., 2018. Self-organization of a biogeomorphic landscape controlled by plant life-history traits. Nat. Geosci. 11 (9), 672–677. https://doi.org/10.1038/s41561-018-0180-y.
Smolders, S., Plancke, Y., Ides, S., Meire, P., Temmerman, S., 2015. Role of intertidal wetlands for tidal and storm tide attenuation along a confined estuary: a model study. Nat. Hazards Earth Syst. Sci. 15 (7), 1659–1675. https://doi.org/10.5194/nhess-15-1659-2015.
Spencer, K.L., Harvey, G.L., 2012. Understanding system disturbance and ecosystem services in restored saltmarshes: integrating physical and biogeochemical processes. Estuar. Coast. Shelf Sci. 106, 23–32. https://doi.org/10.1016/j.ecss.2012.04.020.
Staver, L.W., Stevenson, J.C., Cornwell, J.C., Nidzieko, N.J., Staver, K.W., Owens, M.S., Logan, L., Kim, C., Malkin, S.Y., 2020. Tidal marsh restoration at Poplar Island: II. elevation trends, vegetation development, and carbon dynamics. Wetlands 40, 1687–1701. https://doi.org/10.1007/s13157-020-01295-4/Published.
Stoorvogel, M.M., Temmerman, S., Oosterlee, L., Schoutens, K., Maris, T., van de Koppel, J., Meire, P., Bouma, T.J., 2024a. Nature-based shoreline protection in newly formed tidal marshes is controlled by tidal inundation and sedimentation rate. Limnol. Oceanogr. https://doi.org/10.1002/lno.12676.
Stoorvogel, M.M., van Belzen, J., Temmerman, S., Wiesebron, L.E., Fivash, G.S., van IJzerloo, L., van de Koppel, J., Bouma, T.J., 2024b. Salt marshes for nature-based

flood defense: sediment type, drainage, and vegetation drive the development of strong sediment beds. Ecol. Eng. 207, 107335. https://doi.org/10.1016/j.ecoleng.2024.107335.

Temmerman, S., Meire, P., Bouma, T.J., Herman, P.M.J., Ysebaert, T., De Vriend, H.J., 2013. Ecosystem-based coastal defence in the face of global change. Nature 504 (7478), 79–83. https://doi.org/10.1038/nature12859.

Temmerman, S., Horstman, E.M., Krauss, K.W., Mullarney, J.C., Pelckmans, I., Schoutens, K., 2023. Marshes and mangroves as nature-based coastal storm buffers. Annu. Rev. Mar. Sci. 15, 95–118. https://doi.org/10.1146/annurev-marine-040422.

Temmink, R.J.M., Lamers, L.P.M., Angelini, C., Bouma, T.J., Fritz, C., van de Koppel, J., Lexmond, R., Rietkerk, M., Silliman, B.R., Joosten, H., van der Heide, T., 2022. Recovering wetland biogeomorphic feedbacks to restore the world's biotic carbon hotspots. Science 376 (6593), eabn1479. https://doi.org/10.1126/science.abn1479.

Torfs, H., Mitchener, H., Huysentruyt, H., Toorman, E., 1996. Settling and consolidation of mud/sand mixtures. Coast. Eng. 29 (1–2), 27–45. https://doi.org/10.1016/S0378-3839(96)00013-0.

van den Hoven, K., Kroeze, C., van Loon-Steensma, J.M., 2022. Characteristics of realigned dikes in coastal Europe: overview and opportunities for nature-based flood protection. Ocean Coast. Manag. 222, 106116. https://doi.org/10.1016/j.ocecoaman.2022.106116.

van den Hoven, K., van Belzen, J., Kleinhans, M.G., Schot, D.M.J., Merry, J., van Loon-Steensma, J.M., Bouma, T.J., 2023. How natural foreshores offer flood protection during dike breaches: an explorative flume study. Estuar. Coast. Shelf Sci. 294, 108560. https://doi.org/10.1016/j.ecss.2023.108560.

Van Ledden, M., Van Kesteren, W.G.M., Winterwerp, J.C., 2004. A conceptual framework for the erosion behaviour of sand-mud mixtures. Cont. Shelf Res. 24 (1), 1–11. https://doi.org/10.1016/j.csr.2003.09.002.

Van Putte, N., Temmerman, S., Verreydt, G., Seuntjens, P., Maris, T., Heyndrickx, M., Boone, M., Joris, I., Meire, P., 2020. Groundwater dynamics in a restored tidal marsh are limited by historical soil compaction. Estuar. Coast. Shelf Sci. 244, 106101. https://doi.org/10.1016/j.ecss.2019.02.006.

Van Rijn, L.C., 1990. Chapter 5: Fluid dynamics. In: Van Rijn, L.C. (Ed.), Principles of Fluid Flow and Surface Waves in Rivers, Estuaries, Seas and Oceans. Aqua Publications, Amsterdam, The Netherlands (pp. 5.1 – 5.53).

van Zelst, V.T.M., Dijkstra, J.T., van Wesenbeeck, B.K., Eilander, D., Morris, E.P., Winsemius, H.C., Ward, P.J., de Vries, M.B., 2021. Cutting the costs of coastal protection by integrating vegetation in flood defences. Nat. Commun. 12 (1), 6533. https://doi.org/10.1038/s41467-021-26887-4.

Vermeulen, J., Van Dijk, S.G., Grotenhuis, J.T.C., Rulkens, W.H., 2005. Quantification of physical properties of dredged sediments during physical ripening. Geoderma 129 (3–4), 147–166. https://doi.org/10.1016/j.geoderma.2004.12.040.

Vuik, V., Jonkman, S.N., Borsje, B.W., Suzuki, T., 2016. Nature-based flood protection: the efficiency of vegetated foreshores for reducing wave loads on coastal dikes. Coast. Eng. 116, 42–56. https://doi.org/10.1016/j.coastaleng.2016.06.001.

Walles, B., Brummelhuis, E., van der Pool, J., Wiesebron, L., Ysebaert, T., 2019. Development of benthos and birds in an intertidal area created for coastal defence (Scheldt estuary, the Netherlands). Wageningen Marine Research, Yerseke. https://doi.org/10.18174/475792.

Wang, H., van der Wal, D., Li, X., van Belzen, J., Herman, P.M.J., Hu, Z., Ge, Z., Zhang, L., Bouma, T.J., 2017. Zooming in and out: Scale dependence of extrinsic and intrinsic factors affecting salt marsh erosion. J. Geophys. Res. Earth 122 (7), 1455–1470. https://doi.org/10.1002/2016JF004193.

Weisscher, S.A.H., Baar, A.W., van Belzen, J., Bouma, T.J., Kleinhans, M.G., 2022. Transitional polders along estuaries: driving land-level rise and reducing flood propagation. Nat. Based Sol. 2, 100022. https://doi.org/10.1016/j.nbsj.2022.100022.

Wickham, H., François, R., Henry, L., Müller, K., 2023. dplyr: A Grammar of Data Manipulation. https://dplyr.tidyverse.org. https://github.com/tidyverse/dplyr.

Willemsen, P.W.J.M., Horstman, E.M., Bouma, T.J., Baptist, M.J., van Puijenbroek, M.E.B., Borsje, B.W., 2022. Facilitating salt marsh restoration: the importance of event-based bed level dynamics and seasonal trends in bed level change. Front. Mar. Sci. 8, 793235. https://doi.org/10.3389/fmars.2021.793235.

Winterwerp, J.C., Albers, T., Anthony, E.J., Friess, D.A., Mancheño, A.G., Moseley, K., Muhari, A., Naipal, S., Noordermeer, J., Oost, A., Saengsupavanich, C., Tas, S.A.J., Tonneijck, F.H., Wilms, T., Van Bijsterveldt, C., Van Eijk, P., Van Lavieren, E., Van Wesenbeeck, B.K., 2020. Managing erosion of mangrove-mud coasts with permeable dams – lessons learned. Ecol. Eng. 158, 106078. https://doi.org/10.1016/j.ecoleng.2020.106078.

Wolters, M., Garbutt, A., Bakker, J.P., 2005. Salt-marsh restoration: evaluating the success of de-embankments in north-West Europe. Biol. Conserv. 123 (2), 249–268. https://doi.org/10.1016/j.biocon.2004.11.013.

Ysebaert, T., Meire, P., Coosen, J., Essink, K., 1998. Zonation of intertidal macrobenthos in the estuaries of Schelde and Ems. Aquat. Ecol. 32, 53. https://doi.org/10.1023/A:1009912103505.

Zhou, Z., van der Wegen, M., Jagers, B., Coco, G., 2016. Modelling the role of self-weight consolidation on the morphodynamics of accretional mudflats. Environ. Model. Softw. 76, 167–181. https://doi.org/10.1016/j.envsoft.2015.11.002.

Zhu, Z., Vuik, V., Visser, P.J., Soens, T., van Wesenbeeck, B., van de Koppel, J., Jonkman, S.N., Temmerman, S., Bouma, T.J., 2020. Historic storms and the hidden value of coastal wetlands for nature-based flood defence. Nat. Sustain. 3 (10), 853–862. https://doi.org/10.1038/s41893-020-0556-z.